Carbon Nitride

DOI: 10.1002/anie.201101182

Polymeric Graphitic Carbon Nitride as a Heterogeneous Organocatalyst: From Photochemistry to Multipurpose Catalysis to Sustainable Chemistry

*Yong Wang, Xinchen Wang, and Markus Antonietti**

Keywords:
carbon nitride ·
heterogeneous catalysis ·
mesoporous materials ·
photocatalysis

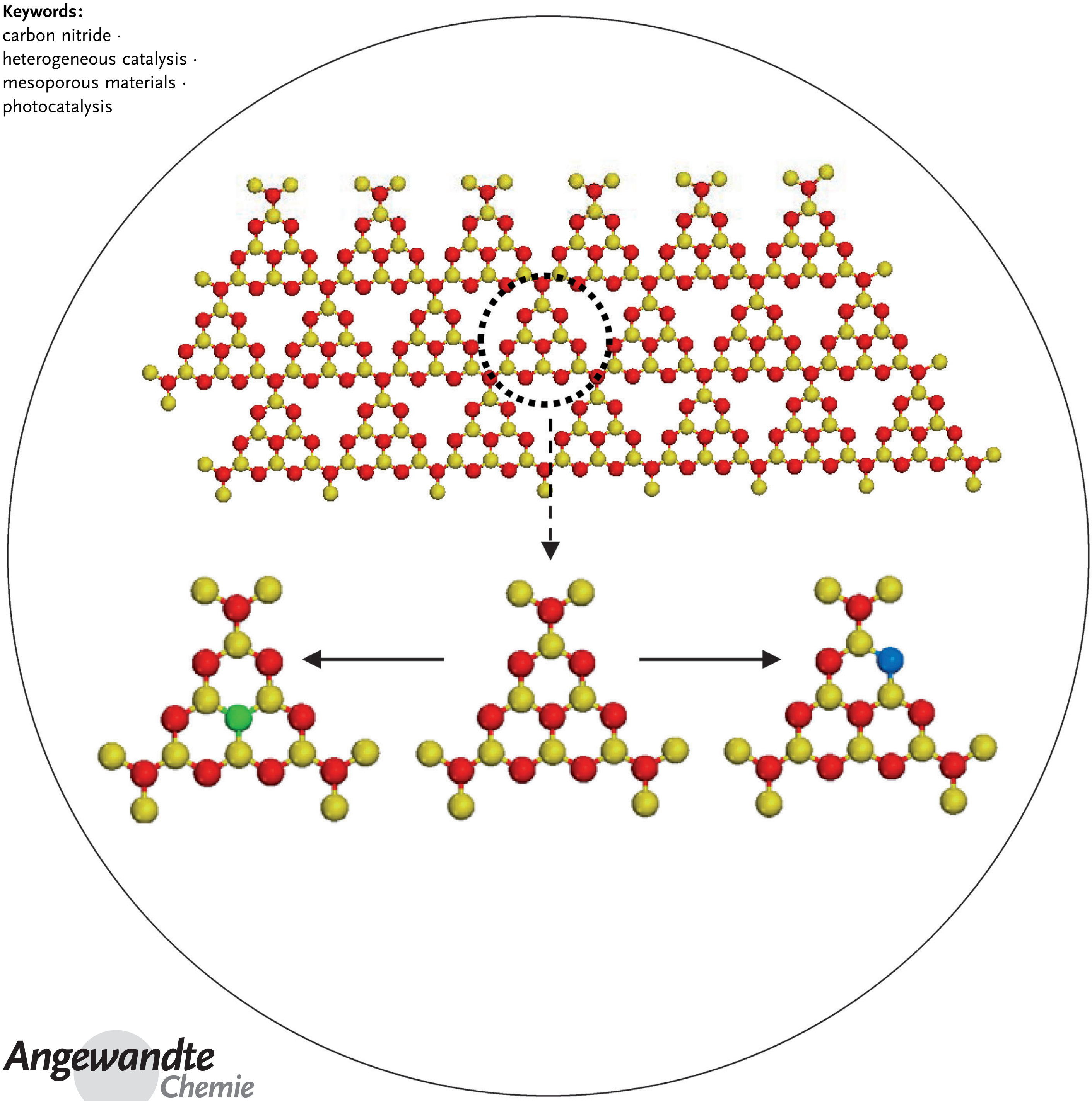

Angewandte
International Edition Chemie

Polymeric graphitic carbon nitride materials (for simplicity: g-C_3N_4) have attracted much attention in recent years because of their similarity to graphene. They are composed of C, N, and some minor H content only. In contrast to graphenes, g-C_3N_4 is a medium-bandgap semiconductor and in that role an effective photocatalyst and chemical catalyst for a broad variety of reactions. In this Review, we describe the "polymer chemistry" of this structure, how band positions and bandgap can be varied by doping and copolymerization, and how the organic solid can be textured to make it an effective heterogenous catalyst. g-C_3N_4 and its modifications have a high thermal and chemical stability and can catalyze a number of "dream reactions", such as photochemical splitting of water, mild and selective oxidation reactions, and—as a coactive catalytic support—superactive hydrogenation reactions. As carbon nitride is metal-free as such, it also tolerates functional groups and is therefore suited for multipurpose applications in biomass conversion and sustainable chemistry.

From the Contents

1. Introduction

Sustainable chemistry focuses on the design of chemical processes that cause minimal environmental impact and it seeks to reduce and prevent pollution at its source.[1–5] Optimization of existing chemical processes together with the development of novel, environmentally friendly processes depend greatly on improvement of catalyst performance.[6] Catalysis thus has a strong impact on the development of modern sustainable chemistry.[7–9] Solid heterogeneous catalysts are convenient for recovering and recycling catalysts from reaction environments, which lead to improved processing steps, better process economics, and environmentally friendly manufacturing.[10,11] Traditional inorganic materials are limited in the nature of their active sites and thus the scope of applications that they can accomplish.[12] Organic polymeric catalysts or catalyst supports have the advantage of flexibility for optimization but traditionally suffer from substantial swelling and stability problems.[13] Another issue is tolerance of the catalytic center against functional organic groups. While traditional catalysts have been optimized for hydrocarbon processing, future biomass-based conversion schemes unequivocally require inertness against most simple functional groups, such as OH, NH_2, COOH, and water. A highly active heterogenous catalytic that meets these requirements could therefore be considered to be a "game changer" and is still eagerly sought after.

A fascinating choice—at least as a starting point—is carbon nitride. It is not new at all and presumably one of the oldest reported polymers in the scientific literature as such. A polymeric derivative was already made by Berzelius and named by Liebig in 1834 as "melon", and is to be regarded as one of the oldest synthetic polymer as such.[14] A more detailed discussion of actual synthetic pathways will be presented below. It is however interesting to note here that this polymeric semiconductor is mainly composed of carbon and nitrogen, and its organic chemistry provides ways to modify its reactivity without having to change the overall composition too much. Indeed, reports on approaching the synthesis of different modifications and the elucidation of the composition and structure of carbon nitride materials abound in the literature.[15–28] Potential applications in energy conversion,[29,30] hydrogen[31–33] and carbon dioxide storage,[34] purification of contaminated water,[35] in solar cells,[36–38] as humidity and gas sensors[39,40] have also been reported.

The so-called g-C_3N_4 is the most stable allotrope of carbon nitride and has attracted much attention in recent years.[12,41–47] The framework topology previously identified in g-C_3N_4 is in fact presumably a defect-rich, N-bridged "poly(tri-*s*-triazine)". As the *s*-triazine ring (C_3N_3) is aromatic, it is expected that a conjugated, two-dimensional polymer of s-triazine would tend to form a π-conjugated planar layers like that of graphite, which has been proven by wide-angle X-ray diffraction (XRD) patterns and SEM and TEM observations.[48–51] The tri-*s*-triazine ring structure and the high degree of condensation makes the polymer possess highly stable with respect to thermal (up to 600 °C in air) and chemical attack (for example, acid, base, and organic solvents) and an appealing electronic structure, being a medium-bandgap, indirect semiconductor.[41,52,53] This allows its direct use in sustainable chemistry as a multifunctional heterogeneous metal-free catalyst, for example in oxidation of hydrocarbons[42,54] and water splitting.[51,55,56]

Interestingly, many organic inorganic compounds or metals could bind or intercalate into the matrix and provide a convenient means of fine-tuning the structure and reactivity of g-C_3N_4, if so desired. Such procedures have already been widely used to control the performance of carbon nitride; examples including protonation,[57] boron,[54] fluorine,[51] and

---

[*] Dr. Y. Wang, Prof. Dr. X. Wang, Prof. Dr. M. Antonietti
Max-Planck Institute of Interfaces and Colloids, Golm, Potsdam (Germany)
E-mail: pape@mpikg.mpg.de

sulfur doping.[58,59] The introduction of functional atoms or groups in the matrix or surface of the carbon nitride undoubtedly greatly improved its performance and expanded applications.

Although there are a few inspiring reviews focused on the selected topic in synthesis and properties of carbon nitride,[29,41,60] a relatively comprehensive and updated review on its role as a organocatalyst is still lacking. In the present Review, we will first give a brief introduction into the general chemistry and properties of carbon nitride. Recent advancements in the modification of carbon nitrides and their applications in sustainable chemistry will then be emphasized.

2. A Brief Development History of Carbon Nitride

As already mentioned, the history of carbon nitride and its precursors can be traced back to the very early days of Berzelius and Liebig in 1834 (Scheme 1).[14] Closer insights into the structure of these compounds were described by Franklin as early as 1922. He introduced the concept of "carbonic nitride" (C_3N_4) and suggested that C_3N_4 might be obtained as the final deamination product of the series of ammonocarbonic acids by heating melon.[61] Pauling and Sturdivant initially suggested a coplanar tri-*s*-triazine unit as the basic structural motif of these polymeric derivatives in 1937.[62] Later, Redemann and Lucas indicated that there is a formal resemblance between melon and graphite in that the molecules are infinitely large and planar. They deduced that the Franklin's carbon nitride closed to a compact condensation product with 21 molecules of 2,5,8-triamino-tris-*s*-triazine, $C_{126}H_{21}N_{175}$.[63] Based on these findings it was stated that one single structure should probably not be assigned to melon as it is more likely a mixture of polymers of different size and architecture.

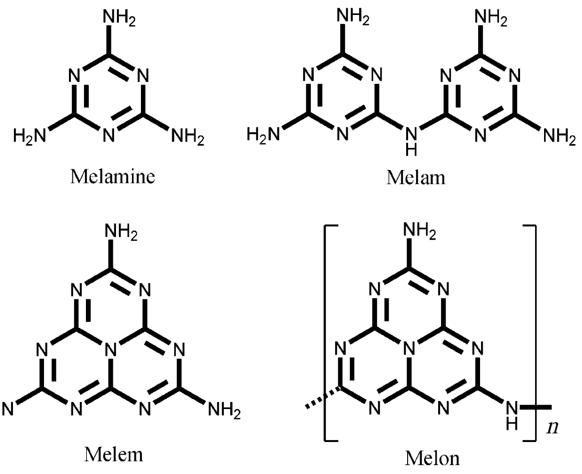

Scheme 1. Carbon- and nitrogen-containing materials obtained from the thermolysis of mercury(II) thiocyanate as described by Liebig.

The above melon-based carbon nitrides had for a long time been forgotten as unconfirmed species. Not only then were researchers challenged by the chemical inertness and low solubility—possibly one reason why their structures remained unclear in detail until today. In 1990s, more than 150 years later, the interest in these compounds blossomed by the theoretical prediction that dense sp^3-bonded C_3N_4 phase (β-C_3N_4) could have extremely high bulk modulus and hardness values comparable with or exceeding that of diamond.[64–68] These results motivated further experimental efforts to synthesize and characterize β-C_3N_4.[69–75]

However, it turned out to be very difficult to prepare single-phase sp^3-hybridized carbon nitride phases because of their low thermodynamic stability.[76] Further theoretical work indicated g-C_3N_4 to be the most stable allotrope at ambient conditions.[67,77–79] The synthesis and characterization of g-C_3N_4 is a challenging task by itself, and to date a large number of different experimental attempts have been made.[17,23,80–87] A very detailed description of the development of these approaches was recently given by Kroke,[29] Antonietti,[41] Blinov,[60] and Matsumoto[88] et al.

Owing to the lack of experimental data, there is a prevailing discussion about the actual existence of a graphitic material with idealized composition C_3N_4 and possible structure models for g-C_3N_4. Inspired by the structure of graphite, triazine (C_3N_3) had been put forward as elementary building blocks of g-C_3N_4 (Scheme 2).[29,44,67,77–79,89–104] However, another possible building block, tri-*s*-triazine (heptazine) rings, which are structurally related to the hypothetical polymer melon,[14,61,105–108] have recently been shown to be energetically favored with respect to the triazine-based modification.[102,109] The tri-*s*-triazine rings are cross-linked by trigonal nitrogen atoms (Scheme 2), and very recent work

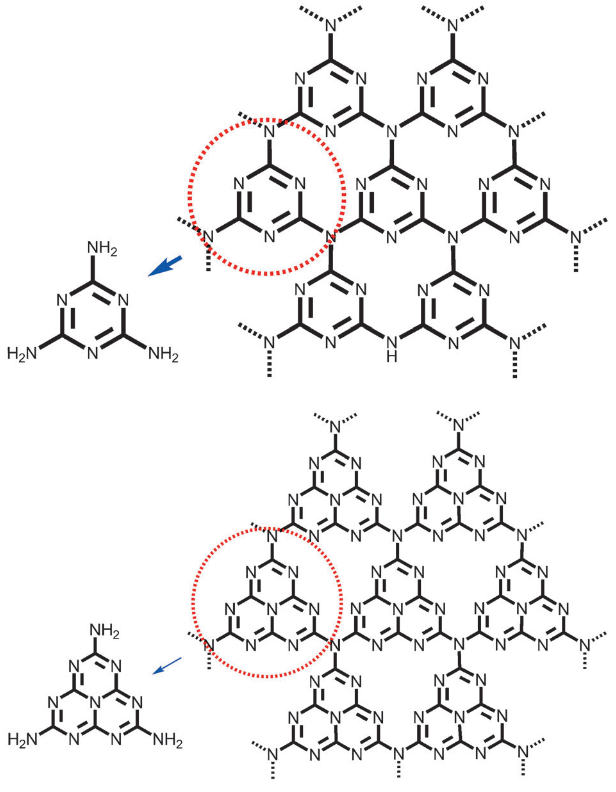

Scheme 2. *s*-Triazine (top) and tri-*s*-triazine (bottom) as tectons of g-C_3N_4.

has shown that indeed the pyrolysis of cyanamide, dicyandiamide, or melamine yields a melon polymer built up from melem units,[45,49,80,81,83,91,102,109–112] confirming that this tecton is the most stable local connection pattern.

Up to now, the condensation pathways of cyanamide to dicyandiamide and later to melamine and all of the other C/N materials described by Liebig were seen as good synthetic strategies to generate slightly defect, polymeric species (Scheme 3). But from the perspective of the fundamental understanding of materials structures, it is still challenging to synthesize a perfect crystalline carbon nitride. The bulk synthesis routes based on these C/N/H-containing compounds have, despite numerous attempts, not yielded the desired, ideally condensed, crystalline C_3N_4 phase, which is widely acknowledged as being a predominantly kinetic problem.[41]

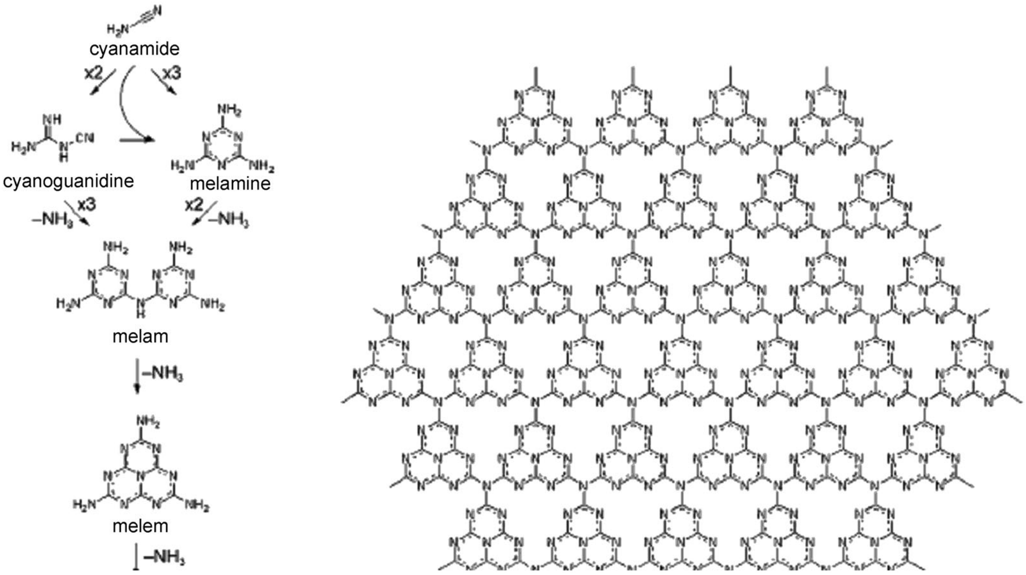

Scheme 3. Condensation reactions of cyanamide to give discrete oligomers, polymers, and extended networks.

The acquisition of accurate data beyond stoichiometry and composition remains largely elusive owing to poor crystallinity and a high degree of disorder of the as-synthesized material. Only a very few exceptions involved the highly textured carbon nitride, but the results are still under discussion. In 2001, Komatsu reported highly crystalline species that was believed to be "high-molecular-weight" melon.[111,112] Schnick and co-workers were able to isolate and identify the crystal structures of heptazine derivatives melem $C_6N_7(NH_2)_3$[81,113] and melam $[(H_2N)_2(C_3N_3)]_2NH$.[110] This work shed light on the argument of possible block units of g-C_3N_4; at the same time the results indicated that the chemical synthesis of high crystal packing of carbon nitride is not impossible. In 2007, McMillan and co-workers reported that conversion of dicyandiamide under high-pressure, high-temperature (HP-HT) conditions indeed yields a crystalline carbon nitride imide phase, $C_2N_2(NH)$.[114] Just recently, the formation of a highly crystalline carbon nitride by a simple self-condensation of dicyandiamide in a salt melt of lithium chloride and potassium chloride has been demonstrated.[80]

In the present context however, we do not have to focus on perfectly crystalline materials, as it turned out in most of the catalytic experiments that the defect-containing, polymeric g-C_3N_4 is far more active. As in most heterogenous catalysis, surface terminations and defects seem to be the real active sites, whereas crystalline perfection only contributes to the bulk properties, such as the graphitic structure, high thermal and chemical stability, and semiconductor electronic structure.[41,60] Furthermore, understanding carbon nitride as a polymer enables diverse synthetic tools to be applied, such as copolymerization with similar tectons, curvature and nanostructure design, or templating to generate high specific surface area. In our opinion, these methods have turned out to be far more valuable than the search for the single crystal.

The potential applications of g-C_3N_4 as an organic semiconductor in materials science and catalysis had been seriously neglected until the discovery of its application as a metal-free catalyst in 2006.[115,116] These reports inspired numbers of efforts toward the development of its new applications; the use of carbon nitride or its modifications in sustainable chemistry now constitutes a forefront of modern carbon nitride chemistry.

3. Properties of Carbon Nitride

3.1. Thermal Stability

Thermal gravimetric analysis (TGA) on g-C_3N_4 reveals that this material is significantly robust and non-volatile up to 600 °C even in the air. A strong endothermal peak appears at 630 °C, paralleled by consecutive complete weight loss, which indicates that the thermal decomposition and vaporization of the fragments started at this temperature. Gillan sealed carbon nitride in evacuated silica ampoules and placed them in a temperature gradient. This study revealed that a very slow sublimation of carbon nitride sets in at 450 °C and increased massively at 650 °C.[117] Complete decomposition of carbon nitrides occurs at 750 °C and results in no residue of the material. This thermal stability is however one of the highest for an organic material and for instance higher than those of typical high-temperature polymers and aromatic polyamides and polyimides. Note that the thermal stability of carbon nitride is somewhat different from different preparation methods in the literature,[49,55,86,117,118] which may be caused by the different degrees of polymerization.

3.2. Chemical Stability

As with graphite, the stacking with optimized van der Waals interactions between the single layers of carbon nitride makes it insoluble in most solvents. No detectable solubility or reactivity of carbon nitride has been observed in conventional solvents, including water, alcohols, DMF, THF, diethyl ether, and toluene.[117] To test the stability and durability of g-C_3N_4 in organic solvents, carbon nitride powder was dispersed in water, acetone, ethanol, pyridine, acetonitrile, CH_2Cl_2, DMF, glacial acetic acid, and 0.1 M NaOH aqueous solution for 30 days. These dispersed carbon nitride samples were then dried at 80 °C for 10 h and then their IR spectra had been measured to compare with the fresh carbon nitride. The IR spectra of the soaked carbon nitride samples were essentially unchanged from that of the fresh material. There are two exceptions: treating g-C_3N_4 in molten alkali metal hydroxides results in a hydroxolysis of the structure. Treatment in concentrated acids on the other hand leads to presumably sheet-like dissolution to give a colloidal dispersion,[57] which however is fully reversible.

3.3. Optical and Photoelectrochemical Properties

The optical properties of carbon nitride were investigated by UV/Vis absorption and photoluminescence experiments. As revealed by the theoretical calculations, polymeric carbon nitride is a typical semiconductor with a bandgap of up to 5 eV, depending on structural variations or adatoms.[119] Indeed, conventional carbon nitride shows the typical absorption pattern of an organic semiconductor with a strongly expressed bandgap adsorption at about 420 nm (Figure 1 a). This is consistent with its pale yellow color, as already reported by a number of authors.[41,53,120]

It is worth noting that the preparation method, including precursors used and condensation temperature slightly effect the absorption edge of carbon nitride, which may be due to the different local structure, packing, and defects formed during the preparation or modification processes.[53,55] For example, different modifications of carbon nitride may lead to a blue-shift (such as protonation[57] or sulfur doping[58]) or red-shift (boron and fluorine doping[51] and copolymerization with barbituric acid[121]) of the adsorption edge (see also Section 4).

Several photoluminescent species have been reported, and some of them exhibit emission in the blue region. It seems that the photoluminescence spectrum sensitively depends on the degree of condensation and the packing between the layers.[41,81,86,120,122] Generally, ordinary polymeric carbon nitride exhibits strong blue photoluminescence at room temperature. The luminescence was observed over a wide range (430–550 nm) and has a maximum at about 470 nm.

The suitable electronic band structure also makes carbon nitride a promising candidate for solar energy converting systems, such as photoelectrochemical cells (Figure 2).[37] Indeed, photocurrent was observed even in the case of bulk g-C_3N_4 under the illumination of visible light ($\lambda > 420$).[37,42,121] The high chemical and thermal stability of carbon nitride makes photoelectrochemical cells stable under an oxygen atmosphere. Furthermore, the electronic band structures of g-C_3N_4 could be tuned by modification of the nanomorphology or doping (Figure 2), which makes the improvement in photocurrent possible. For example, mesoporous carbon nitride (mpg-C_3N_4) can in principle enhance the light harvesting ability owing to its large surface area and multiple scattering effects, and therefore showed an increase in photocurrent.[123] Other modifications, including doping and protonation, can also increase the photocurrent.[37,42,121]

Although the modification of carbon nitride partly improved the photocurrent, it is to be said that at present the photocurrent is still rather low, which is assumed to be due to the grain boundary defects and the inability to synthesize larger domain sizes with current synthetic schemes. Considering different modifications of task-specific carbon nitrides using the rich chemistry of carbon and nitrogen available, we

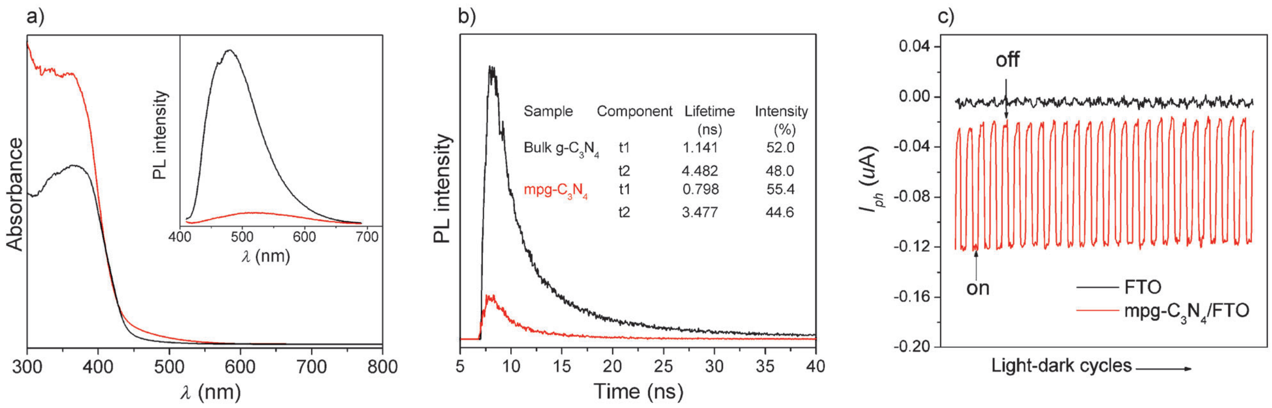

Sample	Component	Lifetime (ns)	Intensity (%)
Bulk g-C_3N_4	t1	1.141	52.0
	t2	4.482	48.0
mpg-C_3N_4	t1	0.798	55.4
	t2	3.477	44.6

Figure 1. a) Diffuse reflectance absorption spectrum and photoluminescence (PL) spectrum (inset) under 420 nm excitation and b) time-resolved PL spectrum monitored at 525 nm under 420 nm excitation at 298 K for bulk g-C_3N_4 (black) and mpg-C_3N_4 (red). c) Periodic on/off photocurrent I_{ph} response of a mpg-C_3N_4 electrode in 0.5 M Na_2SO_4 under zero bias in a two-electrode photoelectrochemical cell.[123] (Reproduced with permission from the American Chemical Society, copyright 2009.)

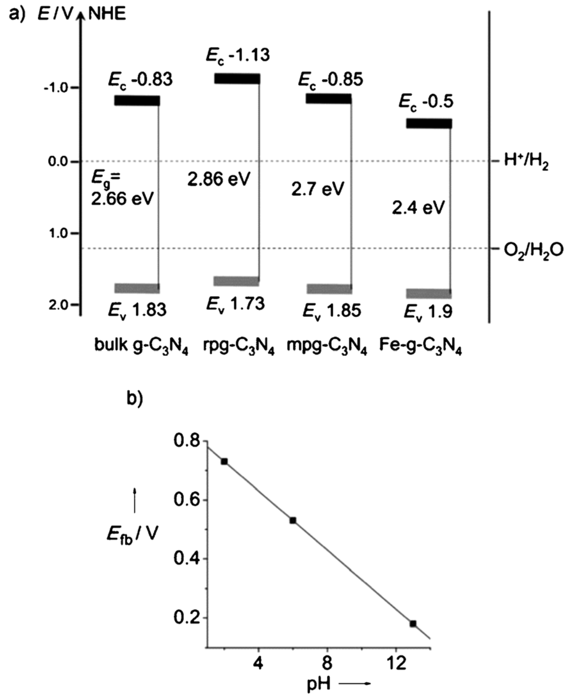

Figure 2. Electronic band structures of different g-C_3N_4 solids. a) The HOMO and LUMO; b) correlation of the flat-band potential (vs. NHE) of mpg-C_3N_4 and pH in 0.1 m KCl aqueous solution.

expect however that this problem can be resolved by future research in this direction.

4. Modifications of Carbon Nitride

4.1. Texture Modification of Carbon Nitride

4.1.1. Synthesis of Mesoporous Carbon Nitride by Nanocasting Techniques

Carbon nitride materials collected directly after self-condensation of organic precursors are bulk materials with a very small surface area, normally below $10\,m^2g^{-1}$. For practical applications of the materials in fields such as catalysts or catalyst supports, the introduction of controlled porosity at the nanoscale in the bulk carbon nitride is mandatory to enhance its function. Starting from a liquid precursor and making a material by condensation enables however a multitude of processing steps unheard of in solid-state chemistry, including printing, stamping, spinning, film casting, molding, templating, and extrusion. For the creation of high specific surface area, nanocasting is advisable.[124]

The first mesoporous g-C_3N_4 (mpg-C_3N_4) was obtained by nanocasting/replication of mesoporous silica matrices, which are well-known from the generation of the corresponding carbon nanostructures.[48,125,126] In a typical synthetic procedure, the silica template and organic precursor (for example cyanamide) were first mixed in aqueous solutions. After removal of water, the resulting composite was subsequently heated for 4 h at 550 °C, ensuring the condensation of the precursor into polymeric C_3N_4. Removing of the silica template with an aqueous NH_4HF_2 solution yielded the carbon nitride replica as a yellow powder. XRD and IR measurements revealed the formation of an extended graphitic carbon nitride structure in the pore walls. By utilizing this "hard template" method, the morphological properties of carbon nitride can be controlled to a certain extent, featuring surface areas between $86\,m^2g^{-1}$ and $439\,m^2g^{-1}$, depending on the weight fraction of silica template.[41,115] Subsequently, ordered mesopore carbon nitrides with different mesostructures have also been synthesized using SBA-15 as a hard template.[127,128]

Other strategies involved the use of ethylenediamine (EDA) and carbon tetrachloride (CTC) as precursors.[30,34,129–131] For example, Vinu et al. reported the synthesis of mesoporous carbon nitride by nanocasting techniques through a simple polymerization reaction between CTC and EDA.[129,130] Their materials featured ordered pores and controlled textual parameters; however, X-ray diffraction measurements showed low crystallinity of the pore walls, while the C/N molar ratio (ca. 5) indicated the loss of the vast majority of nitrogen. However, this is nevertheless relevant for catalysis, as will be discussed below.

4.1.2. Synthesis of Mesoporous Carbon Nitride by using Soft Templates

Nanocasting methods are good as a proof-of-principle, but the extra step involving etching with aqueous ammonium bifluoride (NH_4HF_2) or hydrogen fluoride (HF) is not only hazardous and environmentally unfriendly, but also prohibits further functionalization. Development of reliable and facile strategies for the production of mesoporous materials using "soft templates" carbon and carbon nitrides is therefore of growing interest.[132–134] For thermodynamic and physicochemical reasons, preparing porous materials using soft templates is sometimes still a challenge.[125,135,136]

By introducing holding sequences in the heating program according to the decomposition temperature of the surfactants, nanoparticulate C_xN_y was successfully synthesized using surfactants or amphiphilic block polymers as soft templates, but most experiments yielded a closed pore system, as decomposition of the template at too early a stage enables the resealing of the pores.[137] Triton X-100 was found to be a favorable exception. Nicely developed pore texture which reflects the geometric properties of the original Triton X-100 supermolecular aggregates was observed by TEM, and the nitrogen adsorption isotherms of as-prepared mpg-C_xN_y revealed a BET surface area of $76\,m^2g^{-1}$, while micropores were essentially absent in the materials.

Except Triton X-100, ionic liquids (ILs) are another favorable choice as a soft template for nanostructured carbon nitride solids.[42,137] As a kind of new ionic solvent, ILs offer some distinct physical and chemical properties for high-temperature templating, for example high thermal stability (in some cases in excess of 400 °C) and negligible vapor pressure. Indeed, the ILs gave good nanoporous structures with acceptable porosity. For example, a porous material with a pore size of 5.6 nm, a BET surface of $81\,m^2g^{-1}$ was obtained by using butylmethylimidazolium dicyanamide ionic liquid as a soft template.[137] However, parts of this C,N-based ionic liquid enters the materials upon condensation as a co-monomer, essentially yielding different heteroatom-doped carbon nitride materials. This can be unfavorable, but also can favorably extend the range of applications, depending on the specific chemistry.

It is worth noting that this way a new kind of boron- and fluorine-doped polymeric carbon nitride solid has also been synthesized by using butylmethylimidazolium tetrafluoroborate as a soft template.[42] These doped carbon nitride materials exhibited outstanding mesoporous textural properties, with pore volumes and sizes equal to materials prepared by the above-mentioned hard template routes. For example, the sample CNBF-0.5 exhibits the largest specific Brunauer–Emmett–Teller (BET) surface area of 444 $m^2 g^{-1}$ and a total pore volume of 0.32 $m^2 g^{-1}$, while micropores are again essentially absent in these materials (Figure 3).

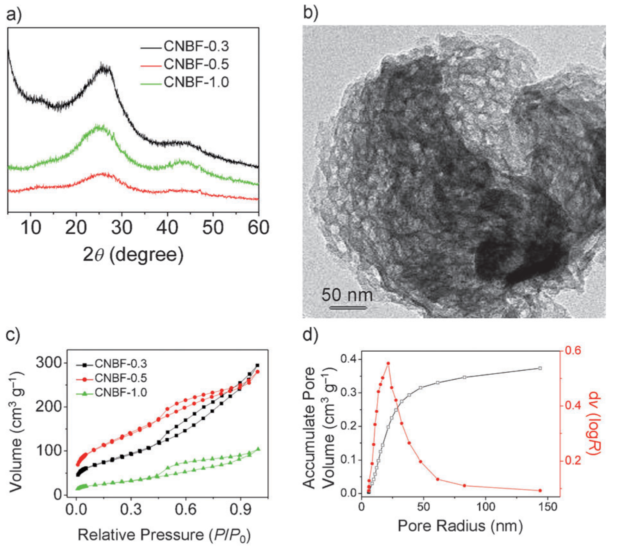

Figure 3. a) XRD patterns of CNBF-*r* (*r* is the mass ratio of $BmimBF_4$/DCDA) for $r = 0.3$ (black), 0.5 (red), or 1.0 (green); b) Typical TEM image of CNBF-0.5; c) N_2 isotherms of the CNBF materials (see (a) for color scheme); d) pore-size sistributions of CNBF-0.3 (black) and CNBF-0.5 (red).

The textural construction was confirmed by analysis of TEM images (Figure 3), which demonstrate the organization of a mesoscale "morel-like" morphology, exhibiting the narrow pore size distribution also confirmed by N_2 sorption studies. Note that these boron- and fluorine-enriched mesoporous materials exhibited excellent catalytic performance for the selective oxidation of cyclohexane (discussed in Section 5).

4.2. Chemical Functionalization of Carbon Nitride

Chemical modification is an effective strategy for tuning physicochemical properties of the parent materials and extends their applications.[138] One way of achieving this control in solid materials is by elemental doping, a method usually used in tailoring the texture and surface chemical properties, as well as the electronic properties of carbon,[139,140] TiO_2,[141,142] and silicon.[143] This heteroatom doping strategy has also been applied to tune the carbon nitride materials. Effects of doping carbon nitride with boron,[54] fluorine,[51] sulfur,[58] and other elements are well-documented.

4.2.1. Post-Functionalization

In terms of the chemical modification of carbon nitrides, post-functionalization or post-treatment to introduce functional groups onto the surface of carbon nitrides is a possible approach. Postfunctionalization has for instance been used in the modification of carbon nanotubes[144,145] and fullerenes[146] and made them suitable for applications. As these carbon nitride materials are rich in nitrogen, direct protonation while adding a counterion is a very convenient modification route. Indeed, carbon nitride could be reversibly protonated by stirring with 37% HCl for 3 h at room temperature.[57] After protonation, the almost unchanged features of the XRD patterns (two feature diffraction peaks at around 27° and 13°) supports the preservation of the original C/N matrix (Figure 4).

The protonation of carbon nitride tuned the electronic bandgaps and led to higher ionic conductivity of carbon nitride. Adding protons also improved its dispersion in aqueous solutions which makes characterization and processing easy. Furthermore, this method can be further extended through a simple counteranion exchange.

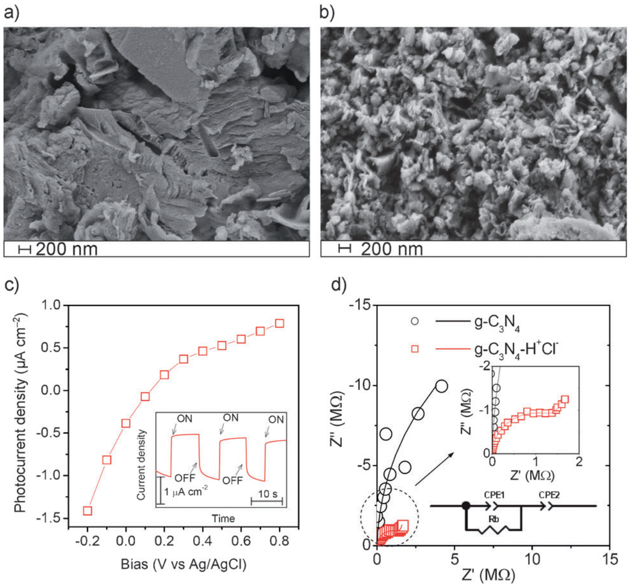

Figure 4. SEM images of a) as-prepared and b) regenerated $g-C_3N_4$. Scale bars are 200 nm; c) photocurrent–applied-potential dependence at a regenerated C_3N_4/ITO electrode in 0.1 M KCl under visible light. Inset: Photocurrent biased at −0.2 V; d) Nyquist impedance plots for $g-C_3N_4$ and $g-C_3N_4-H^+Cl^-$ (data points) and simulation (lines). Frequency range 106–103 Hz, perturbation signal 100 mV. Inset: Expanded view of the dotted area and the equivalent circuit. The calculated resistances (R_b) before and after protonation were about 28 and 1.5 MΩ, respectively.[57] (Reproduced with permission from the American Chemical Society, copyright 2009.)

Another example of post-functionalization is a sulfur-doped carbon nitride.[58] Cheng and co-workers reported a sulfur-doped carbon nitride (g-$C_3N_{4-x}S_x$) by treating fresh g-C_3N_4 at 450 °C in a gaseous H_2S atmosphere. Homogeneous sulfur doping was observed in the energy-filtered TEM image, which also revealed a strong S contrast (Figure 5 b). The structural details on the incorporation of sulfur into the C/N framework were obtained with XPS and XANES spectroscopy, which suggested that C–S bonds formed in g-$C_3N_{4-x}S_x$ by substituting sulfur for lattice nitrogen (Figure 5 d). In a similar fashion to protonation, sulfur doping also modified the surface area and the morphology of g-C_3N_4, which is as such relevant for catalytic applications.

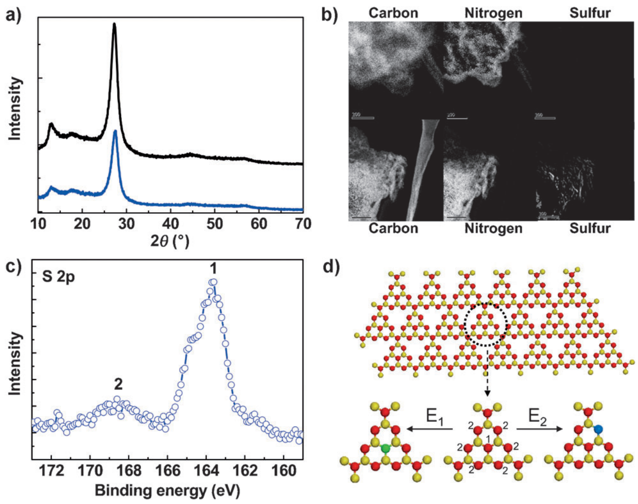

Figure 5. a) XRD patterns of C_3N_4 (black) and $C_3N_{4-x}S_x$ (blue); b) energy-filtered TEM images of carbon, nitrogen, and sulfur in C_3N_4 and $C_3N_{4-x}S_x$; c) high-resolution XPS spectrum of sulfur recorded from pristine surface of $C_3N_{4-x}S_x$; d) atomic structure model of a perfect graphitic C_3N_4 sheet consisting of melem units, and two melem units with a substitutional nitrogen atom at different periodic sites by sulfur atom. C yellow, N red, S green (site 1), S blue (site 2).[58] (Reproduced with permission from the American Chemical Society, copyright 2010.)

4.2.2. *In Situ Synthesis of Modified Carbon Nitride*

The second strategy involves the in situ synthesis of modified carbon nitride. In this strategy, additive was added before the lattice was formed, and heteroatoms such as boron and fluorine or other grafts were incorporated into the matrix in situ. One typical example is the synthesis of boron- and fluorine-containing mesoporous carbon nitride polymers, as mentioned above.[42] This approach employs the ionic liquids with BF_4^- as the anion from the many different ionic liquids. This BF_4^- anion entered the C–N condensation process during the self-condensation of an organic precursor, for example dicyandiamide.

In an analogous study, the ionic liquid 1-butyl-3-methylimidazolium hexafluorophosphate ($BmimPF_6$) was selected as a mild phosphorus source for doping carbon nitride. This phosphorus doping provides not only a much better electric conductivity of up to four orders of magnitude but also an improvement in photocurrent generation by a factor of up to 5 (Figure 6).

This ionic-liquid-based method can be extended to incorporate other heteroatoms by changing the anion or cation of the ionic liquids into C,N-based materials, which opens up the possibility of designer material synthesis for specific applications.

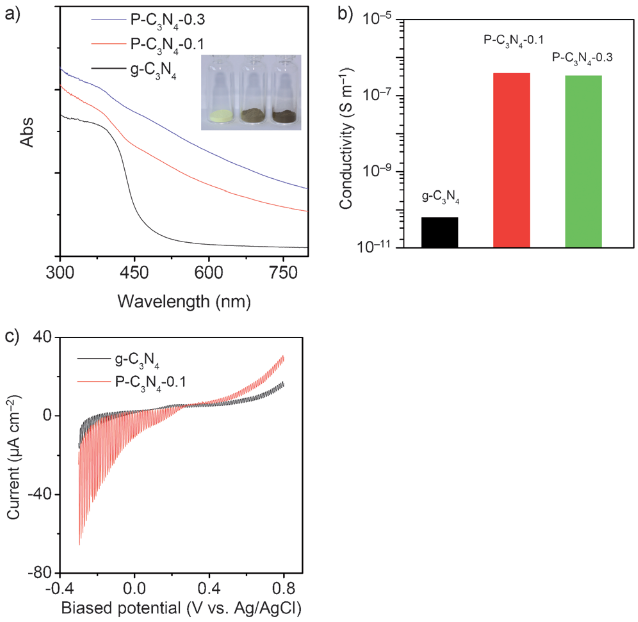

Figure 6. a) UV/Vis spectra and b) electrical conductivity of P-doped and pristine g-C_3N_4. Inset: photographs of g-C_3N_4 (left), P-C_3N_4-0.1 (middle), and P-C_3N_4-0.3 (right); c) current–potential curve of P-doped and pristine g-C_3N_4 photoelectrodes in 0.1 M aqueous KCl under chopped visible light ($\lambda > 420$ nm, 150 W Xe lamp, chopping frequency 0.5 Hz, scan rate 10 mV s^{-1}).[57] (Reproduced with permission from the American Chemical Society, copyright 2010.)

In a further set of experiments, carbon nitride materials separately doped with boron and fluorine were synthesized using aminoborane and ammonium fluoride as co-monomers. Fluorination was accomplished on the freshly thermally induced condensation of dicyandiamide.[51] Both XPS and solid-state MAS NMR spectroscopy indicated the incorporation of fluorine atoms into the CN matrix as C–F bonds (Figure 7), which results in a partial conversion of sp^2 C to sp^3 C in the carbon nitride matrix and may further lead to a lower plane order of the materials. Compared with unmodified g-C_3N_4, the graphitic stacking as revealed by XRD is much weakened after fluorination (Figure 7).

The use of aminoborane-modified g-C_3N_4 by replacing the carbon atoms in the network by boron, forming a planar layered configuration like melon. Here, the planar heterocyclic macrocycle structure is still present, while the boron sites on the surface might act as strong Lewis acid sites, thus complementing the basic nitrogen sites in bifunctional catalysis.[54] Structural details on the incorporation of boron into the C/N matrix were obtained with ^{11}B solid-state MAS NMR and XPS experiments. The ^{11}B NMR spectrum gives two peaks, which indicates two different positions in the

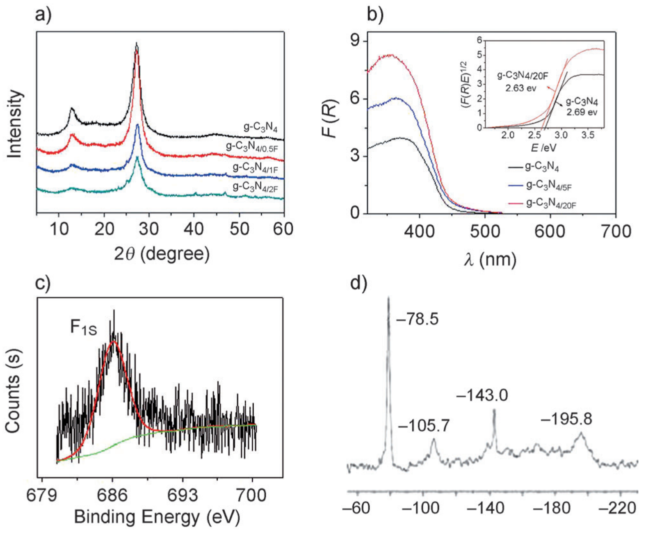

Figure 7. a) XRD patterns and b) UV/Vis spectrum of g-C_3N_4 and CNF-*x*, and the optical bandgap (E_g) of g-C_3N_4 and CNF-2.0 (b, inset); c) XPS spectra of CNF-2.0; d) ^{19}F solid-state MAS NMR spectra of CNF-2.0.[51] (Reproduced with permission from the American Chemical Society, copyright 2010.)

framework structure, say as corner boron and bay boron (Figure 8).

Other modification methods include the copolymerization of the nitrogen precursor (for example dicyandiamide) with other organic additives, such as barbituric acid.[121] In contrast to inorganic modification methods, the modified carbon nitride based on organic copolymerization shows a remarkable red-shift of the optical absorption from 470 to 750 nm with increasing barbituric acid content, which would allow photochemical application of wavelengths in which the solar photon flux is maximal (Figure 9).

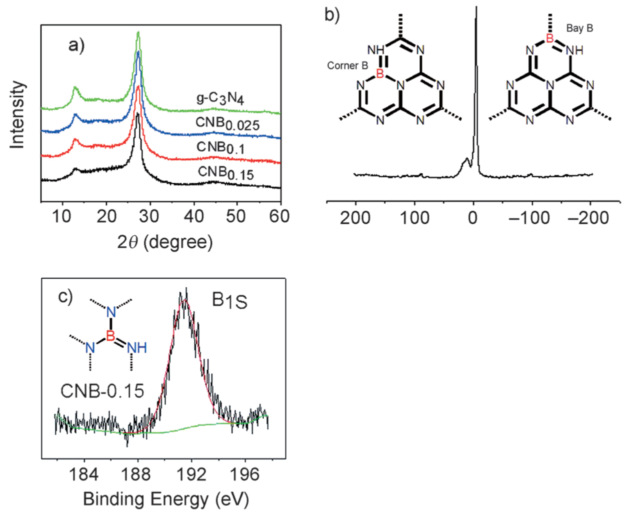

Figure 8. a) XRD patterns of the B-doped and pristine g-C_3N_4; b) ^{11}B solid-state MAS NMR spectra of $CNB_{0.15}$ (inset: the building unit of C_3N_4 with B-doping at the bay-carbon site (right) and at the corner-carbon site (left)); c) XPS spectra of $CNB_{0.15}$.[54] (Reproduced with permission from the Royal Society of Chemistry, copyright 2011.)

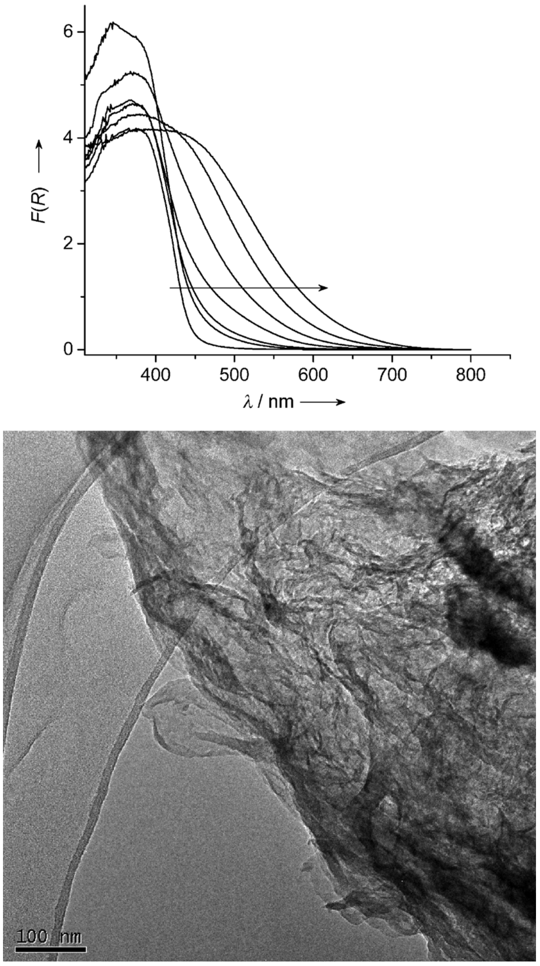

Figure 9. Top: UV/Vis diffuse-reflectance spectra of g-C_3N_4 and CNB samples (in the direction of the arrow: g-C_3N_4, $CNB_{0.05}$, $CNB_{0.1}$, $CNB_{0.2}$, $CNB_{0.5}$, $CNB_{1.0}$, and $CNB_{2.0}$). Bottom: a typical TEM image of the lamellar mesostructure of $CNB_{0.05}$.[121]

Apart from covalent atom doping, metal salts can also be dissolved into the nitrogen cavities of the matrix of g-C_3N_4. Kawaguchi and co-workers first reported the synthesis of metal-modified carbon nitride in 1995.[118] They suggested that the proposed structure of carbon nitride contains a hole that is surrounded by three amino radicals in a unit cell. This hole was expected to allow incorporation of certain chemical species, for example metal atoms. They heated the $[(C_3N_3)_2(NH)_3]_n$ powder with metal chloride (for example $AlCl_3$ or $ZnCl_2$) at 500 °C for one hour, which led to a yellowish material. The IR spectrum of the metal-modified material was very similar to the host carbon nitride material, which supported the retention of the host framework. Although the broadening and weakening of (002) diffraction had been observed in the metal-loaded material, its position did not move, which suggested a similar graphitic stacking structure as the host material. Within the nitrogen "pots", large amounts (up to 59 wt %) of metal can be partly incorporated. No diffraction of metal (Al or Zn) or metal salt ($AlCl_3$ or $ZnCl_2$) was observed in the XRD patterns. This result suggested that the metal has been homogeneously inserted into the matrix of the host material. On the other hand, only minor amounts of the counterions are found in the matrix, which means that the negative charges have to be taken up by the CN framework.

In a similar fashion, iron ions were also found to be included into the carbon nitride matrix without destroying the graphitic structure of the host.[147] XRD patterns and optical absorption spectra studies indicated that the incorporation of iron into the matrix of carbon nitride strongly modified the electronic properties of carbon nitride, and provided systems with additional new functionality (Figure 10).

5. Applications of Carbon Nitride

Carbon nitride has interesting properties, such as good accessibility at a low price, a high thermal and chemical stability, and amenability to chemical modification, which makes it suitable for a range of applications. Even in this early stage, carbon nitrides together with their modifications have already found numerous applications in relevant fields of chemistry.[41,42,53,148] In the following section, we will summarize some of the recent, most remarkable examples.

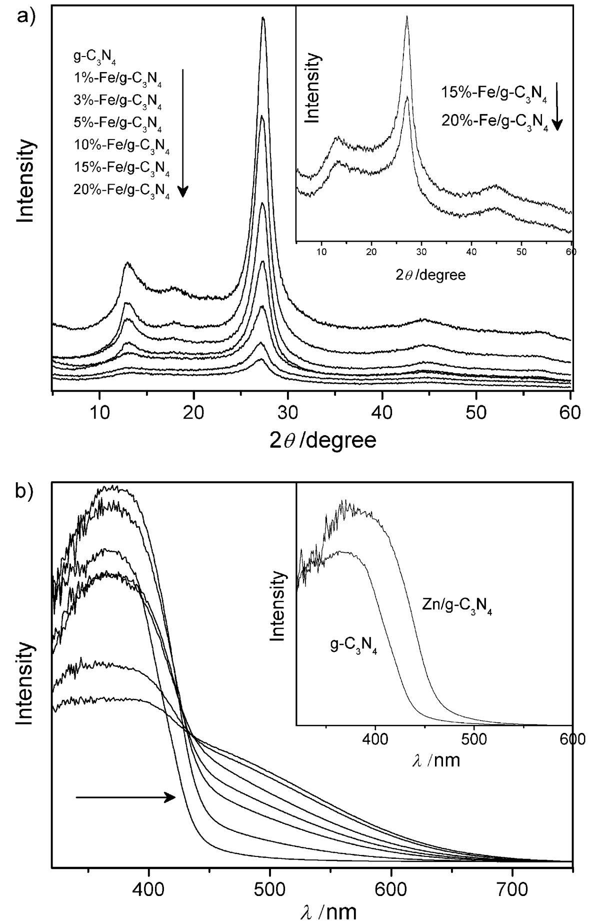

Figure 10. Comparison of a) XRD spectra and b) optical absorption spectra for $g\text{-}C_3N_4$ with those of $Fe/g\text{-}C_3N_4$ hybrids with varying Fe content. Inset in (a): enlarged XRD spectra of 15% and 20% $Fe/g\text{-}C_3N_4$. Arrow direction in (b): $g\text{-}C_3N_4$, 1%, 3%, 5%, 10%, 15%, and 20% $Fe/g\text{-}C_3N_4$. The bandgap is shifted towards lower energies in the hybrid materials. Inset in (b): optical spectrum of 10% $Zn/g\text{-}C_3N_4$, which also demonstrates narrowing of the $g\text{-}C_3N_4$ bandgap by the metal inclusion.[147]

5.1. Carbon Nitride as a Photocatalyst for Water Splitting

Direct water splitting using a photocatalyst with visible light is a silver bullet to produce hydrogen fuel, thus converting sunlight into storable and transportable energy.[149,150] To date, studies on heterogeneous photocatalysis have mainly focused on the development of materials with a sufficiently small bandgap and suitable band positions for overall water splitting, accompanied by adequate stability for practical applications.[151] Most of these semiconductor materials were solely inorganic and metal-based, comprising metal oxides, nitrides, sulfides, and phosphides and their mixed solid solutions.[152] Owing to its structural and electronic properties, $g\text{-}C_3N_4$ contains all the prerequisites required for a heterogeneous photocatalyst; it has the correct electronic structure with an appropriate bandgap of 2.7 eV, corresponding to an optical wavelength of 460 nm. This bandgap is sufficiently large to overcome the endothermic character of the water-splitting reaction, which normally requires four photons with a average energy of 1.23 eV. Moreover, $g\text{-}C_3N_4$ exhibits an appropriate microstructure, with surface termination with defects and nitrogen atoms for electron localization or for anchoring the active sites. Most importantly, both the HOMO and the LUMO encompasses the oxidation and reduction potential of water (Scheme 4), that is, the electron vacancy ("hole") in the HOMO is sufficiently reactive to oxidize water to oxygen, while the electron in the LUMO has enough reduction potential to reduce water to hydrogen.[37] This is a rare if not lucky case for an organic semiconductor structure. For example, a recent breakthrough was achieved by the use of this material as an efficient and inexpensive photocatalyst for water splitting under visible light in the presence of external redox agents.[53,153]

A $g\text{-}C_3N_4$ catalyst exhibits activities for water reduction into H_2 or water oxidation into O_2 in the presence of a proper

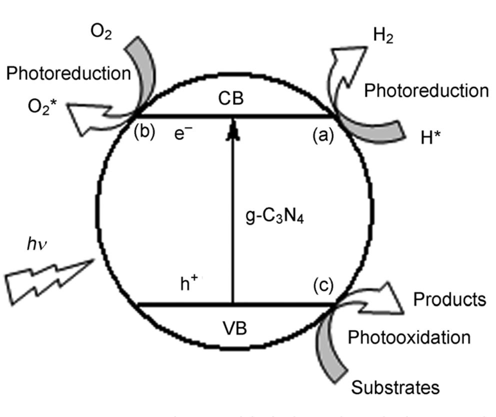

Scheme 4. Strategies to realize visible-light-induced photocatalysis. a) Hydrogen evolution from water; b) photochemical activation of O_2; c) photocatalytic oxidation or degradation of organic substrates.

sacrificial electron donor or acceptor, even in the absence of noble metal catalysts (Figure 11).[53,153] To date however, efficient and stable H_2 evolution could only be achieved by modification of g-C_3N_4 with a small amount of co-catalyst, such as Pt. This is presumably due to kinetic effects, as splitting of a Pt−H bond is much less kinetically hindered than splitting of an N−H bond.

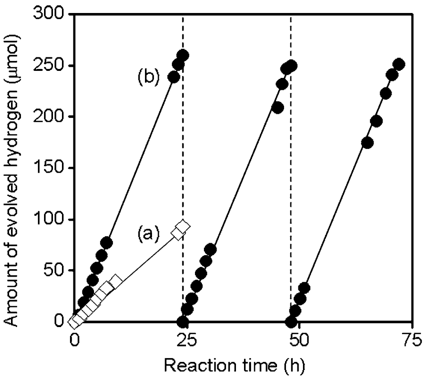

Figure 11. Stable hydrogen evolution from water by g-C_3N_4. A typical time course of H_2 production from water containing 10 vol% triethanolamine as an electron donor under visible light (of wavelength longer than 420 nm) by a) unmodified g-C_3N_4 and b) 3.0 wt% Pt-deposited g-C_3N_4 photocatalyst. The reaction was continued for 72 h, with evacuation every 24 h (dashed line).

The estimated quantum efficiency of g-C_3N_4 in the initial experiment was still rather low (approximately 0.1% with irradiation of 420–460 nm), even with the help of Pt. We can attribute that to charge recombination by inner grain boundaries and a nanostructure that is not optimized for the lifetime of the photoexited charge pairs. The amenability to mass preparation and chemical modifications of carbon nitride provides further possibilities to adjust the electronic and optical properties of this material.

A high dispersion of co-catalysts on the g-C_3N_4 surface is favorable (Table 1).[153] For example, the complex bis(1,5-cyclooctadiene)platinum, [Pt(cod)$_2$], was found to be a better precursor than H_2PtCl_6 because of better access of [Pt(cod)$_2$] to the g-C_3N_4 surface, which caused a better dispersion of Pt nanoparticles on g-C_3N_4. Modification with RuO_2 can improve the stability against the self-decomposition of g-C_3N_4 and improves the O_2 evolution activity.[153] Au/g-C_3N_4 prepared by a deposition–precipitation method also shows improved photocatalytic activity owing to the formation of tight gold–semiconductor heterojunctions effectively promoting the transfer of charge from light-exited g-C_3N_4.[154] Recently, Ye and co-workers reported that the carbon nitride polymer sensitized with N-doped tantalic acid showed a high photocatalytic activity and good stability for hydrogen evolution from an aqueous methanol solution under visible-light irradiation, and up to 4.8% of the apparent quantum yield was achieved at 420 nm.[155]

Table 1: Photocatalytic H_2 evolution activities of g-C_3N_4 modified with various metal co-catalysts.[a]

Entry	Co-catalyst[b]	Steady rate of H_2 evolution [µmol h^{-1}]
1	Ru	2.1
2	Rh	1.6
3	Pd	5.7
4	Ir	0.2
5	Pt	7.3
6	Au	3.7

[a] Reaction conditions: 0.1 g catalyst, aqueous triethanolamine reaction solution (100 mL), xenon lamp (300 W) light source with cutoff filter, top-irradiation reaction vessel. [b] 0.5 wt% loaded by an in situ photodeposition method.

It can be expected that the modification of textural structure of g-C_3N_4 can in principle enhance the light harvesting ability of the materials owing to its large surface and multiple scattering effects. Indeed, the efficiency of hydrogen production from the photochemical reduction of water could be improved by 8.3 times by introducing mesoporosity into g-C_3N_4 (Table 2).[123]

Table 2: Textural properties and photocatalytic activity of Pt/mpg-C_3N_4 for the hydrogen evolution reaction with visible light.[a]

Entry	Catalyst	Surface area [m^2 g^{-1}]	H_2 evolution rate [µmol h^{-1}]	TOF[b] ×100 [h^{-1}]
1	mpg-$C_3N_{4/0.2}$	67	149	27
2	mpg-$C_3N_{4/0.5}$	126	142	26
3	mpg-$C_3N_{4/1.0}$	235	124	23
4	mpg-$C_3N_{4/1.5}$	373	69	13
5	g-C_3N_4	8	18	3
6[c]	g-C_3N_4	10	19	3

[a] For reaction conditions, see Ref. [123]. [b] TON = turnover number.

As mentioned in Section 4, the electronic structure of g-C_3N_4 could be easily adjusted by doping with heteroatoms. For example, the UV/Vis spectrum indicated that fluorine doping gave rise to a decrease in bandgap from 2.69 eV for g-C_3N_4 to 2.63 eV for CNF-2.0 (for a sample with about 3 at% fluorine in the structure; Figure 7). These band changes brought about by fluorine doping are expected to modify the redox properties and promote heterogeneous photocatalysis. Indeed, the H_2 evolution of CNF-0.5 was about 2.7 times higher than that of unmodified g-C_3N_4.[51] Another typical example is the modification of the polymeric subunits by copolymerization with barbituric acid.[121] These copolymerization products show a remarkable red-shift of optical absorption compared to g-C_3N_4 from 470 to 750 nm with increasing barbituric acid content, and an improvement in H_2 evolution activity, both under UV irradiation and especially with visible light. The maximal H_2 evolution activity comes from the most weakly doped sample, which shows a 4.5-fold higher activity than that of unmodified g-C_3N_4.

Very recently, Cheng and co-workers found that the sulfur-doped carbon nitride has an electronic structure with an increased valence bandwidth in combination with an elevated conduction band minimum and a slightly reduced

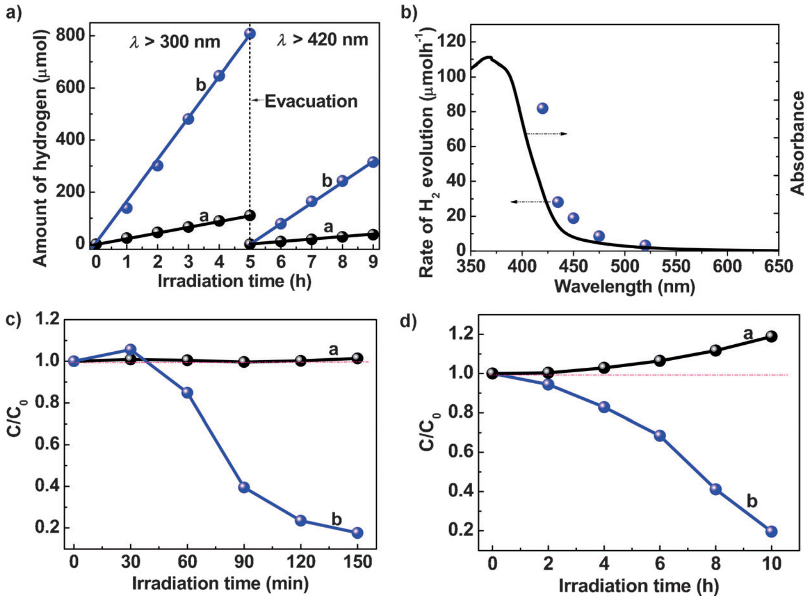

Figure 12. a) A typical time course of hydrogen evolution from water containing 10 vol% triethanolamine scavenger by a) Pt-deposited C_3N_4 and b) $C_3N_{4-x}S_x$ under $\lambda > 300$ and 420 nm, respectively; b) dependence of hydrogen evolution on wavelength by $C_3N_{4-x}S_x$. For comparison, a UV/Vis absorption spectrum of $C_3N_{4-x}S_x$ is also given. c, d) Activity comparison of the photooxidation process for phenol by C_3N_4 (black) and $C_3N_{4-x}S_x$ (blue) under $\lambda > 300$ and 400 nm illumination, respectively.[58] (Reproduced with permission from the American Chemical Society, copyright 2010.)

absorbance (Figure 12).[58] Collectively, these features result in a unique electronic structure that is highly efficient in promoting visible-light photoreduction. This sulfur-doped carbon nitride shows improved photocatalytic activity evolution from an aqueous triethanolamine solution; the photoactivity of H_2 evolution is 7.2 and 8.0 times higher than that of bare g-C_3N_4 for more than 300 nm and for 420 nm, respectively.

Following a related strategy, our group found that a sulfur-mediated synthesis offers an effective approach to modify the texture, optical and electronic properties, and photoreduction and photooxidation.[59] Contrary to other modifications, sulfur-mediated synthesis even lowers the HOMO of the organic semiconductor structure, that is, makes it more stable and therefore the hole in the band structure more oxidative.

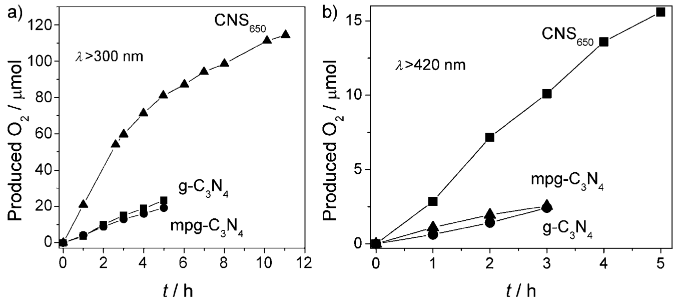

Figure 13. Oxygen evolution by g-C_3N_4, mpg-C_3N_4, and CNS_{650} as a function of time under a) UV and b) visible-light illumination.[59] (Reproduced with permission from the Royal Society of Chemistry, copyright 2011.)

In perfect agreement with these general quantum-chemical considerations, the water oxidation reaction has been achieved at a moderate rate even with only sulfur-mediated carbon nitride without the aid of cofactors (Figure 13). This material is therefore a stronger oxidation agent.

Another promising strategy to extend the photoresponse of carbon nitride to the visible region is to harvest visible light by adsorbed dyes. In this strategy, the dyes act as antenna to absorb and transfer the light energy into the reaction system. In case of appropriately chosen band positions, the photochemical reactions could be initiated through the electron transfer from the excited states of the dye into the conduction band of carbon nitride, leaving the hole well-separated at the dye structure. For example, Domen and coworkers deposited magnesium phthalocyanine (MgPc) to the mpg-C_3N_4 which expands the absorption to the Q band (Figure 14).[156] The as-obtained MgPc/Pt/mpg-C_3N_4 showed stable photocatalytic evolution of hydrogen from an aqueous solution containing TEOA as a sacrificial reagent, resulting in a quantum efficiency of about 5.6% at 420 nm. It is worth noting that the photocatalytic test gave hydrogen evolution even when irradiated at a wavelength longer than 600 nm.

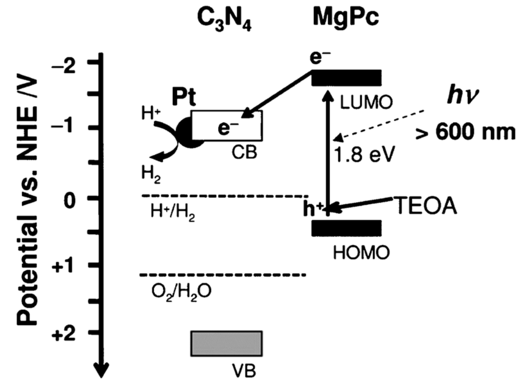

Figure 14. Electron–hole separation in MgPc/Pt/mpg-C_3N_4 photocatalysts. Band positions of mpg-C_3N_4 were determined by photoelectron emission spectroscopy in air and UV/Vis diffuse reflection spectroscopy (DRS).[156] (Reproduced with permission from the Royal Society of Chemistry, copyright 2010.)

5.2. Carbon Nitride as a Catalyst for the Oxidation Reaction

Catalytic oxidation is an important method for bringing functionality into petroleum-based feedstocks, and it is often the first step to high-value fine chemicals, agrochemicals, and pharmaceuticals.[157] Traditional methods of many fine-chemical oxidations involve stoichiometric quantities of toxic and expensive metal reagents and oxidants.[158,159] For economic and environmental reasons, the oxidations using transition metals as catalysts and permanganate or dichromate as oxidants are regarded as typical examples of unsatisfactory processes that need immediate replacement.[160] The ideal system for sustainable oxidation is the use of molecular oxygen or hydrogen peroxide as the primary oxidant together with recyclable metal-free catalysts in nontoxic solvents. In the development of metal-free oxidation catalysis, carbon nitride is a key catalyst and it can be anticipated that in the near future the practical oxygen oxidations will be associated to the use of carbon nitride. Recent work has indeed shown that carbon nitride or its modifications are suitable metal-free catalysis in oxidation of for example alkanes,[42,51,54] olefins,[161] and alcohols.[56]

5.2.1. *Oxidation of Alkanes*

The conversion of alkanes into oxygen-containing compounds is one of the most important and fundamental transformations in industrial chemistry.[6] Higher alkanes and alkyl aromatic hydrocarbons can be oxidized by heating them under oxygen at rather high temperatures through a radical-chain autooxidation.[162] However, the autooxidation is characterized by a lack of selectivity. Therefore, industrially performed catalytic oxidation reactions often suffer from drawbacks such as poor selectivity owing to over-oxidation, lack of catalyst recycling, and negative environmental impact because of the use of toxic metal catalysts.[162,163]

Phenol is an important commodity chemical.[164,165] In industry, most phenol has been produced from benzene by the three-step cumene process, which generates high amounts of waste.[166] The ideal process should be the direct oxidation of benzene to phenol with clean oxidants, such as molecular oxygen or hydrogen peroxide (Scheme 5).[167] In this regard, it was recently found that carbon nitride is indeed an active metal-free photocatalyst for the high selectivity direct oxidation of benzene to phenol under mild conditions.[168]

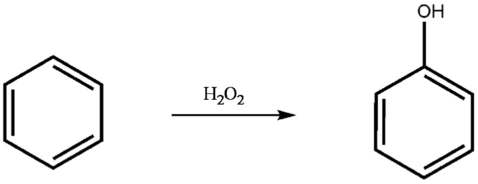

Scheme 5. Direct oxidation of benzene to phenol.

Using hydrogen peroxide as a clean oxidant, at a reaction temperature of 60 °C and under the irradiation of visible light ($\lambda > 420$ nm), fluorine-doped carbon nitrides showed improved activities compared to bare g-C_3N_4. With g-C_3N_4 as catalyst, phenol was formed with a very low turnover frequency (TOF) of 0.006 h^{-1}, which can be enhanced to a TOF of 0.125 h^{-1} using CNF-2.0.[51] Notably, the TOF could be greatly improved by using iron-doped carbon nitride.[154,168] For example, under the same reaction conditions, a TOF of 14.84 h^{-1} was achieved by using Fe-g-C_3N_4/SBA-15 as photocatalyst.

Oxidation of cyclohexane to cyclohexanone is another reaction of industrial important, as cyclohexanone is intermediate in the production of caprolactam and adipic acid, which are used to manufacture of nylon 6 and nylon 66, respectively.[169] The industrial process used cobalt naphthanoate as catalyst and acetic acid as solvent. Operating at a temperature of about 150 °C, selectivity in the range 70–90 % at 5 % conversion are typically achieved.[42,162,170] Recently, boron- and fluorine-enriched carbon nitride was found to promote the oxygenation of cyclohexane with a selectivity of over 90 % at conversions of about 1–8 %. Notably, CNBF-1.0 afforded 100 % selectivity towards the formation of cyclohexanone at 5.3 % conversion.[42]

Other alkanes have also been subjected to oxidation in the presence of carbon nitride catalysts, including toluene, ethylbenzene, and some substituted benzylic aromatics (Scheme 6). The activity of bulk g-C_3N_4 is very low in the oxidation of toluene and ethylbenzene, while doping of boron atoms in the matrix of carbon nitride promotes the catalytic oxidation activity of carbon nitride. For instance, the g-C_3N_4 itself gave minor conversion of 2 % in the oxidation of toluene, whereas $CNB_{0.15}$ gave a conversion up to 6.3 % at 100 % selectivity toward benzaldehyde.[54]

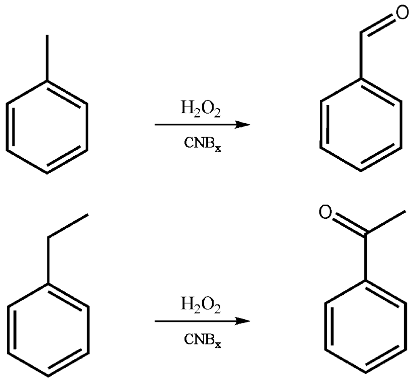

Scheme 6. Oxidation of toluene and ethylbenzene using boron-doped carbon nitride.

This high selectivity toward benzaldehyde or acetophenone is very relevant to industrial applications. In industry, the conversion of toluene has to be kept at less than 4 % to attain 70 % selectivity of benzaldehyde and to avoid the formation of carboxylic acid; however, heavy-metal catalysts as well as high temperature above 200 °C are used. Thus, it seems that a boron-doped carbon nitride could be a feasible solution. The main limitations are maintenance of high selectivity at a conversion above 8 % and avoidance of catalyst deactivation.

From the environmental point of view, reactions based on the use of oxygen as oxidizing reagent, forming water as a byproduct, will be even a more preferable process. It seems that bare carbon nitride is inefficient in promoting inert hydrocarbon (for example cyclohexane) oxidation by oxygen,[54] which is presumably due to its rather mild oxidation potential as determined by its HOMO position. Nevertheless, oxidation of hydrocarbons with an activated benzylic position went smoothly, even with O_2 as the oxidant. Again, the boron-doped carbon nitrides show improved catalytic activity, but even bare carbon nitride gave good conversions and high selectivity using molecular oxygen as clean oxidant (Table 3).

Table 3: Oxidation with molecular oxygen of substituted aromatics to ketones using $CNB_{0.15}$ as metal-free catalyst.[a]

Entry	Substrate	Main Product	BDE[b]	T [°C]	Conv. [%]	Sel. [%]
1	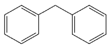	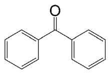	81	160	20.3	95.1
2	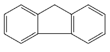	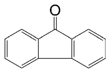	80	130	45.7	> 99.0
3[c]	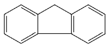	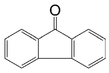	80	130	28.8	> 99.0
4	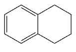	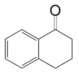	83	130	72.2	87.5
5	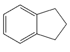	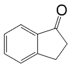	82	115	36.7	> 99.0

[a] Reaction conditions: 1 mmol substrates, O_2 pressure 1 MPa, 50 mg catalyst, 4 mL acetonitrile, reaction time 24 h. [b] a_{C-H} bond dissociation energy from the literature. [c] Using $g-C_3N_4$ as a catalyst.[54]

Although $g-C_3N_4$ or its modifications can in principle catalyze the oxidation of alkanes, the conversion rates are in general very low. Considering the importance of alkane oxidation in industry, much effort still has to be devoted to optimize $g-C_3N_4$ or its modifications as catalysts, promoters, and to optimize reaction conditions.

5.2.2. Oxidation of Olefins

Classical alkene oxidation methods described in the literature are also far from being environmentally benign and significant amounts of undesirable by-products form.[171] For example, even using an enzyme (P450LM2, a rat liver microsomal enzyme) as catalyst, the oxidation of cyclohexene produces cyclohexene oxide and 2-cyclohexen-1-ol in almost equal amounts.[172] In recent years, the model systems that have been developed based on metalloporphyrins seems effective, but the oxidative degradation of the metalloporphyrin catalysts makes them impractical for routine oxidative catalysis, either in academic labs or in industry.[173]

During our continuing studies into selectivity and sustainable oxidation, we recently found that carbon nitride is also an efficient catalyst for the (partial) selective oxidation of alkenes.[161] In the oxidation of cyclohexene, exceptionally high selectivity toward allylic substitution was found by using molecular oxygen as the oxidant. Representative data are given in Figure 15. From the trend indicated in Figure 15, the alternative reaction channel towards cyclohexene oxide is minor, and the final oxidation product would be cyclohexene-2-one. The formation of the allylic products 2-cyclohexene-1-one and 2-cyclohexene-1-hydroperoxide show the preferential attack of the activated C–H bond over the C=C double bond in the oxidation of cyclohexene.

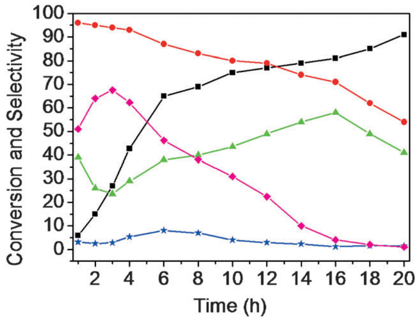

Figure 15. Cyclohexene conversion and selectivity in allylic oxidation and epoxidation products with the reaction time at 110 °C and 1 MPa p_{O_2}. ■ conversion of cyclohexene, ● selectivity of allylic oxidation products, ▲ selectivity of 2-cyclohexene-1-one, ◆ selectivity of 2-cyclohexene-1-hydroperoxide, ⋆ selectivity of cyclohexene oxide.

5.2.3. Oxidation of Alcohols

The oxidation of primary alcohols to aldehydes is another elementary reactions that is of fundamental importance in both the laboratory and commercial procedures.[174–176] Many oxidations of this type are carried out using corrosive and stoichiometric oxygen donors, such as chromate or permanganate, and generally transition-metal catalysts.[177,178] In recent years, heterogeneous photocatalysis has developed into a promising method for a number of chemical reactions that use sunlight.[179,180] As mentioned above, $g-C_3N_4$ has an appropriate bandgap of 2.7 eV (the top of the valance band is 1.4 V and the bottom of the conduction band is −1.3 V versus the normal hydrogen electrode, respectively).[53] This feature allows its direct use in photochemical activation of O_2 and organic compounds in which $g-C_3N_4$ was used as a photocatalyst to absorb light, with the generated charge couple to activate oxygen, for instance for the oxidation of benzene.[51,168]

This photocatalysis system can be easily extended to other oxidation reactions, for example to the oxidation of alcohols.[56] Indeed, our recent work shows that light-excited mesoporous $g-C_3N_4$ can activate molecular oxygen for the oxidation of alcohols to aldehydes/ketones with high selectivity.[56] Thus $mgp-C_3N_4$ catalyzes the oxidation of benzyl alcohol to benzaldehyde with more than 99 % selectivity and 57 % conversion under visible-light irradiation for 3 h at 100 °C (Table 4). A study on the effect of substitution on the aromatic ring shows both the electron-withdrawing and electron-donating substituent enhanced the rate of the reaction (Table 4).

Further electron spin resonance (ESR) experiments suggested the formation of the $^{\bullet}O_2^-$ radical by electron transfer from photoactivated $mpg-C_3N_4$ under visible-light irradiation, while the hole directly dehydrogenates the alcohol (oxidative dehydrogenation).

Table 4: Selective oxidation of alcohols.

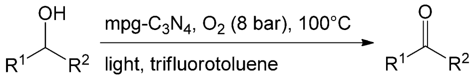

	R^1	R^2	*t* [h]	Conv. [%]	Sel. [%]
1	pentyl	H	3	57	> 99
2	pentyl	CH_3	3	77	> 99
3	4-methylphenyl	H	3	86	90[a]
4	4-chlorophenyl	H	3	79	> 99
5[b]	4-methoxyphenyl	H	1.8	100	95[c]
6	4-methylbenzoate	H	3	80	> 99
7	$PHCH{=}CH_2$	H	3	92	64[d]
8	pentyl	CH_3	5	35	> 99
9	pentyl	cyclopropyl	3	32	90[e]

[a] Acid (10%) was formed. [b] 4-Methoxybenzylalcohol 0.65 mmol. [c] Acid (5%) was formed. [d] Benzaldehyde (36%) was detected. [e] 1-(1,2-Dicyclopropyl-2-phenylethyl)benzene (10%) was formed.

5.2.4. Oxidation of Heteroatoms

Apart from C–H and O–H oxidation, N–H oxidation is of considerable interest as it allows generation of a number of active nitrogen containing compounds as intermediates of various chemically and biologically significant molecules, for example drugs.[181,182] Under the illumination of visible light, mpg-C_3N_4 can also promote the oxidation of amines into imines, which then undergo consecutive reactions. Under optimized conditions, complete conversion of benzylamine into N-(benzylidene)benzylamine was obtained in 3.5 h. Note that this strategy could be successfully extended to other substrates, such as heterocyclic amines containing nitrogen and sulfur atoms, which usually poison most metal catalysts. Specifically, a simple and efficient synthesis of benzoxazoles, benzimidazoles, and benzothiazoles could be realized through a one-pot synthesis by this photocatalytic cascade reaction with high yields (Table 5).[183]

Table 5: One-pot aerobic coupling synthesis of benzoxaoles, benzimidazoles, and benzothiazoles.[183] [a]

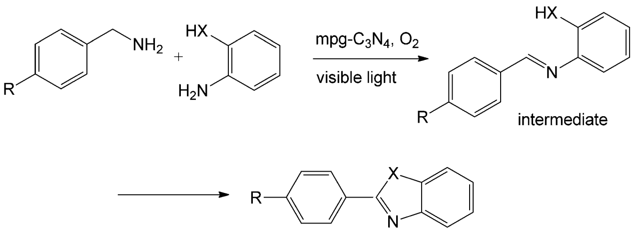

Entry	R	X	*t* [h]	Conv. [%]	Sel. [%]
1	CH_3	O	5	99	69
2	H	O	5	99	75
3[c]	H	O	5	99	24
4	Cl	O	5	70	74
5	CH_3	NCH_3	4	97	92
6	H	NCH_3	5	99	98
7	Cl	NCH_3	5.5	98	91
8	OCH_3	S	4	96	97
9	H	S	5	91	92
10	Cl	S	5.5	97	93

[a] Reaction conditions: substituted benzylamine (1 mmol), mpg-C_3N_4 catalyst (50 mg), 2-aminophenol (2-aminothiophenol or *o*-phenylenediamine; 3 mmol), CH_3CN (10 mL), 100°C, O_2 (0.5MPa). [b] Conversion and selectivity were based on benzylamines. [c] 80°C; using the main product of 2-hydroxybenzoimine.

5.2.5. Photodegradation of Pollutants

The oxidation of the organic pollutants into CO_2, water, and other non-hazardous compounds using O_2 as a clean oxidant is one of the few effective approaches to remove organic pollutants rapidly and environmentally friendly.[184] Recently, Zou and co-workers are able to degrade methyl orange (MO) and rhodamine B (RhB) using g-C_3N_4 as a metal-free photocatalyst.[55] Their comparison studies showed that the photodegradation activity of MO over g-C_3N_4 is mainly attributed to reduction process initiated by photogenerated electrons (Scheme 4), while the degradation of RhB over g-C_3N_4 mainly originated from the oxidation by the photogenerated hole. Boron doping for g-C_3N_4 can improve dye adsorption and light absorption and therefore promote the photodegradation of RhB.[43] The same group also fabricated a C_3N_4-TaON composite photocatalyst by the milling–heat-treatment method. This organic–inorganic heterojunction performed well in the photooxidation of RhB; the good performance resulted from the suitably matching conduction and valance band levels that improved the separation efficiency of photogenerated electron–hole pairs (Figure 16).[185]

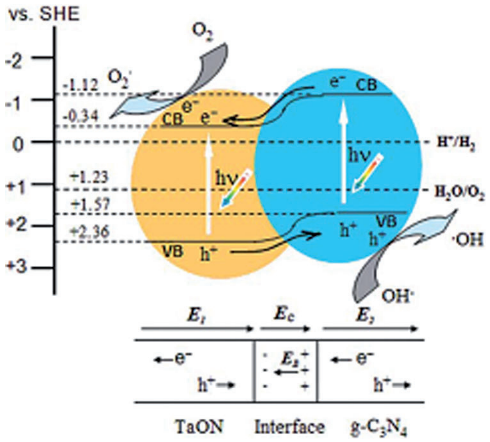

Figure 16. Electron–hole separation and transport at the visible-light-driven organic-inorganic composite photocatalyst interface and in both semiconductors. E_C is the contact electric field for the two materials; E_B is the potential barrier in the interfacial depletion layer ($E_B < E_C$ during a photocatalytic reaction); E_1 and E_2 are the internal electric fields induced by the redistribution of the spatial charges in TaON and C_3N_4 particles, respectively.[185] (Reproduced with permission from the Royal Society of Chemistry, copyright 2010.)

5.3. Applications in Hydrogenation Reactions

An organic semiconductor that can photochemically liberate hydrogen can of course also run the inverse reaction, a hydrogenation reaction. Owing to the kinetic hindrance of splitting covalent organic bonds discussed before, it helps to anchor an appropriate metal nanoparticle such as Pd on the surface of mpg-C_3N_4, thus creating the semiconductor–metal heterojunction Pd@mpg/C_3N_4. The high number of nitrogen atoms in the networks of carbon nitride favors the tight coordination and thus stabilization of metal particles, which is expectedly much higher than in corresponding carbon-supported noble-metal catalysts.

One recent study has shown this quite illustratively: highly-dispersed Pd nanoparticles were introduced as a functional moiety into a mpg-C_3N_4 framework (Figure 17).[186] All of the Pd particles were about 3 nm in size, well-separated from each other, and stable throughout the consecutive reactions. The hybrid material, Pd@mpg/C_3N_4, was subsequently used as a catalyst for the hydrogenation of phenol.

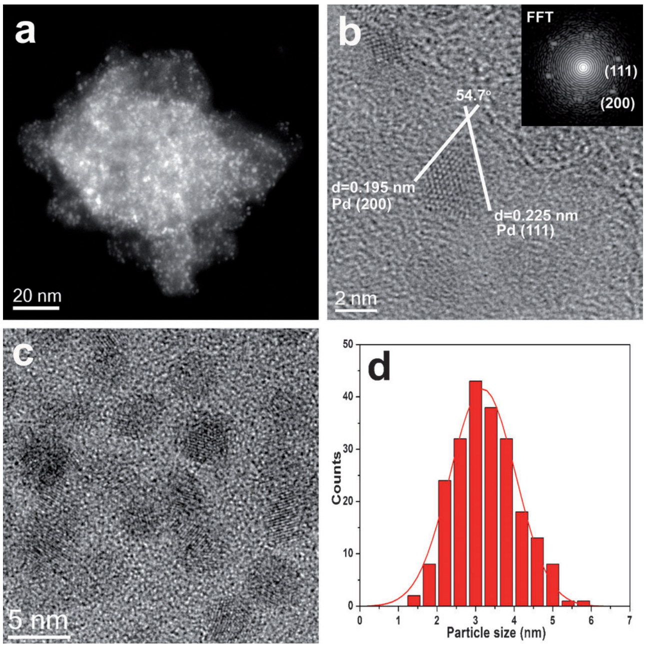

Figure 17. a) STEM, b) HRTEM, c) TEM, and d) particle size distribution (PSD) of Pd@mpg-C_3N_4. Inset in (b): local fast Fourier Transform (FFT).[186] (Reproduced with permission from the American Chemical Society, copyright 2010.)

Prior research on the one-step hydrogenation of phenol to cyclohexanone showed that cyclohexanone is, under standard conditions, a reactive intermediate and was easily further hydrogenated to cyclohexanol, and high selectivity (> 95 %) at elevated conversion (> 80 %) is a great challenge.[165,187,188] Pd@mpg-C_3N_4 was shown to be highly active in hydrogenation and promoted the selective formation of cyclohexanone even under an atmospheric pressure of hydrogen and under aqueous conditions. For example, the catalytic hydrogenation of phenol with 5 mol % Pd@mpg-C_3N_4 in water at 65 °C proceeded with 99 % conversion in 2 h and more than 99 % selectivity for cyclohexanone. The observed reaction rates are generally much higher than those obtained with a classical Pd@C complex, which also gives low selectivity toward cyclohexanone in general and requires the use of additives.[165,189]

Significantly, the Pd@mpg-C_3N_4 catalyst can also be successfully applied to other hydroxylated aromatic compounds with both high conversion and selectivity (> 99 %). Hydrogenation of hydroquinone and pyrocatechol yielded the synthetically very valuable hydroxycyclohexanones. Interestingly, in the case of resorcinol, the obtained product is not hydroxycyclohexanone but the reductive dehydration product cyclohexanone. The high selectivity towards ketones was attributed to the phenol being adsorbed in a nonplanar fashion over basic sites, which gives rise to cyclohexanone (Scheme 7). The interaction of phenol with the surface through the hydroxy group to form strong O−H···N or O−H···π interactions was also regarded as a factor that affected the selectivity.

5.4. Applications as a Basic Catalyst

The development of new basic solid materials is a rapidly expanding area. The incorporation of nitrogen atoms in the texture of polymers and carbon materials gives rise to basic function which dictates the basic catalytic performance of the material. Vinu and co-workers reported the use of highly ordered mesoporous carbon nitride nanoparticles with very large surface areas as basic catalysts for the transesterification of keto esters.[130] The catalyst is highly active and affords a high yield of the corresponding esters in a short time. The same group also demonstrated that gold nanoparticles deposited into N-containing carbon materials can be used as a highly active, selective, and recyclable heterogeneous catalyst for coupling benzaldehyde, piperidine, and phenylacetylene to the corresponding propargylamine, which is otherwise generally catalyzed by using strong bases such as butyllithium, organomagnesium reagents, or lithium diisopropylamide (Scheme 8).[190]

5.5. Application in NO Decomposition

Platinum and palladium are effective catalysts for NO_x reduction, but these noble metals are expensive.[191] Zhu and co-workers recently reported that g-C_3N_4 is a promising candidate in environmentally friendly catalysis for NO decomposition. The g-C_3N_4 itself is active for NO decom-

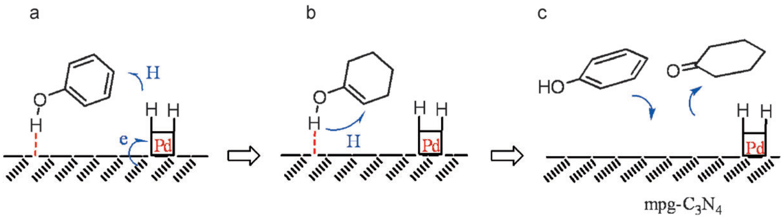

Scheme 7. Possible reaction mechanism of phenol over Pd@mpg-C_3N_4. (Reproduced with permission from the American Chemical Society, copyright 2011.)

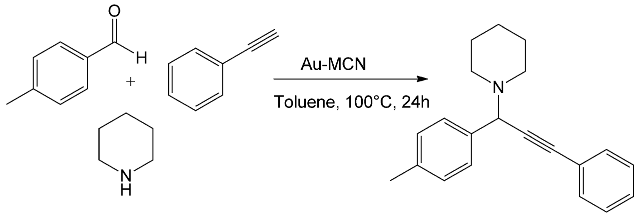

Scheme 8. Catalytic activity of gold-nanoparticle-encapsulated mesoporous carbon nitride in the three-component coupling reaction of benzaldehyde, piperidine, and phenylacetylene for the synthesis of propargylamine.

position but with a low conversion. Enhanced conversion was observed when metal ions such as Zn or Au were introduced in the matrix of carbon nitride (Table 6).[192]

Table 6: NO conversion measured from the investigated catalysts at different temperatures.

Catalyst	NO Conversion [%] 400 °C	450 °C	475 °C	500 °C
g-C_3N_4	0.14	3.46	5.03	15.06
g-C_3N_4*[a]	2.14	18.58	33.33	46.25
Zn-g-C_3N_4	10.83	32.37	48.31	69.40
Au-g-C_3N_4	26.88	23.01	26.59	41.05

[a] g-C_3N_4 was synthesized in basic medium prior to the calcination step.

5.6. Activation of π-Bonds and Aromatic Systems

It was already indicated above that g-C_3N_4 not only activates benzene but also favorably interacts with the various double- and triple-bond reactants.[193] In the cited research, g-C_3N_4 was employed as an effective catalyst for the cyclotrimerization of various nitriles into triazine derivatives and the cyclization of functional alkynes. Cyclotrimerizations of triple bonds are usually very exothermic reactions because they result in the formation of an aromatic system, but such reactions are rarely realized practically because of very high activation energies. Using carbon nitride catalysis, slow reactions, with however moderate to high yields, were observed. It was speculated that while alkenes were activated by electron donation (as is the case for benzene), nitriles interacted with the edges of the C_3N_4 sheets by multiple hydrogen bonding, which provided the catalyst with a very marked substrate selectivity. This was exemplified by the fact that pyrazine carbonitrile was one of the fastest reacting nitriles, while benzonitrile, which has very similar electronic properties and steric hindrance, did not react. Interestingly, the different catalytic modes develop differently with degree of condensation and with optimization of packing. While electronic properties are best for a structure with optimal condensation and not too small structural features, all catalysis reactions that rely on functional groups and edge termination are more efficient with less-ordered, polymeric carbon nitride species and higher surface areas.

Friedel–Crafts (FC) acylation is a typical aromatic C–H activation process. Mesoporous samples of C_3N_4 with varying surface area were analyzed for this specific reaction,[115] and it turned out that the reactivity essentially depends on both the surface area and an optimal degree of condensation. The major advantage of such a metal-free catalysis is that it inherently allows the presence of functional groups in the reactants or leaving groups; such functional groups usually passivate the metal catalyst. The use of carboxylic acids or alcohols as electrophiles lies at the heart of current efforts to render Friedel–Crafts reactions more sustainable, which had previously proved to be rather difficult.[33,194,195] In contrast, the use of mpg-C_3N_4 as a catalyst indeed allowed such a flexible reactant choice. In particular, OH or NH_2 groups could be used as leaving groups, thus allowing for an effective low-temperature alkylation with alcohols or quarternary amines or even a cyanation with urea.[116] Scheme 9 depicts some of these unusual reaction pathways promoted by carbon nitride.

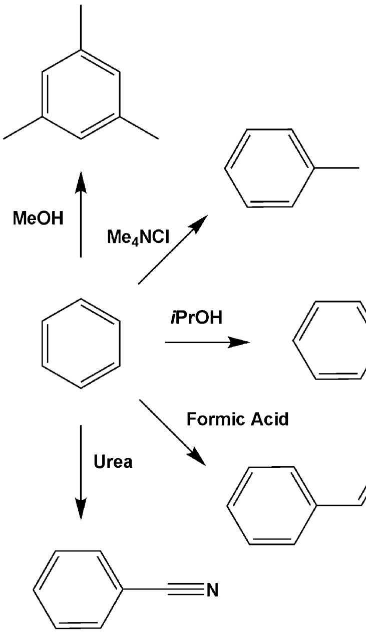

Scheme 9. Some possible Friedel–Crafts-type reactions catalyzed by mpg-C_3N_4 using sustainable electrophiles.

For the Friedel–Crafts reaction, tempering carbon nitride at 600 °C and an increase in organization and condensation seemed to improve the catalytic activity, which was interpreted in that the semiconductor properties drive the reaction by electron transfer to the aromatic system.

It is interesting to see that many of these reactions employing new functionalities for reaction indeed appear to be biomimetic or "enzyme-like", and it is an interesting question as to why C_3N_4 especially is suited for those reactions. One answer may be that a whole number of cyanide-based, nitrogen-rich, conjugated organic molecules, such as nucleic acids and porphyrins, are "molecular fossils" that existed before life begun.[196]

6. C_xN_y Beyond C_3N_4

A necessary and even highly relevant question is if g-C_3N_4 is in any way peculiar, or if this is just one specific case of a broader range of heterogenous organocatalyst. In our opinion, experiments already surely point to the second possibility. There are many ways to substitute carbon by nitrogen in graphite or nanotubes in a regular fashion, and the name "carbon nitrides" can stand for a much larger family of related compounds (say C_3N_3, C_3N_2, C_3N, C_5N, $C_{10}N_3$, etc.), all being potentially condensed from appropriate monomers. This opens new possibilities to form catalytic polymers, scaffolds, and solid materials with new and protentially exciting chemical reactivities.

In some of the applications discussed above, enhanced thermal treatment beyond the stability point and/or copolymerization of carbon nitrides already lowered the nitrogen contents substantially, but nevertheless resulted in highly active catalysts (see for example Refs [129,130]). Another well documented case to complement this family is the so-called "nitrogen-doped carbons", where just minor parts of the carbon framework are replaced by nitrogen. Nitrogen-doped carbon materials are already known to act as metal-free catalysts for oxygen reduction (for some recent contributions, see Refs [197–199]), but still on a less competitive level. Following the present concepts, we described the (metal-free) synthesis of nitrogen-doped carbon materials by heating non-volatile ionic liquids featuring dicyanamide anions to temperatures of 1000 °C.[200,201] Carbon materials with nitrogen contents as high as 10.4 wt% were obtained with an electronic conductivity and oxidation stability superior to pure graphitic carbon.[200,202] These observations go well with the many other positive observations of improving electronic and mechanical properties of bulk carbon materials by N-doping.[203–206] In that work, it was also shown that the density of states at the Fermi level, $D(E_F)$, and the work function will increase linearly with increasing nitrogen content, creating a metal-like conductivity. As nitrogen also improves the HOMO position towards higher nobility, N-doped carbon materials were already called "noble carbons" (as it compares with the effect of for example, chromium in noble steel). The combination of nobility, base character, and metallic behavior can indeed be regarded as an excellent starting point for a variety of catalytic applications.

In this context, simple (nitrogen-rich) nucleobases were used as effective functional comonomers in ionic liquid condensation, and N-doped carbon materials with more than 14 wt% nitrogen were obtained.[207] This corresponds to a formal "C_6N". This metal-free catalyst was cast into a mesoporous structures and turned out to be highly active for the electrochemical reduction of oxygen (ORR), with activities in alkaline solution that were competitive to Pt@C, the classical fuel cell catalyst (Figure 18 a)

This case illustrates well the case of N-doped carbons, as without metal-like conductivity and high chemical inertness, application in a fuel cell reaction would be impossible. Furthermore, the system turned out to be insensitive against methanol spillover (Figure 18 b), the classical weakness of all Pt-based catalysts, which is naturally absent for all carbon materials. A C,N-based electrocatalyst continues to work, while the Pt-based catalyst is poisoned and dies.

7. Conclusions and Outlook

Since the first use of g-C_3N_4 as a metal-free heterogeneous catalyst in 2006,[115,116] thenumber of studies on the catalytic, electrocatalytic, and photocatalytic performance of carbon nitride are steadily increasing. In this Review, we have discussed the elucidation of its peculiar structure and characteristics, discussed different pathways for its modification, and presented applications in sustainable chemistry. It is the peculiarities of modified carbon nitrides that make them heterogeneous organocatalysts, that is, they catalyze reactions by organic interactions and activation. Furthermore, carbon nitride is a medium-bandgap semiconductor, with both the HOMO and LUMO position in a range which makes it a mild electron transfer agent with powerful chemical potential.

As mentioned above, in many examples carbon nitride or its modifications have provided new opportunities in practical

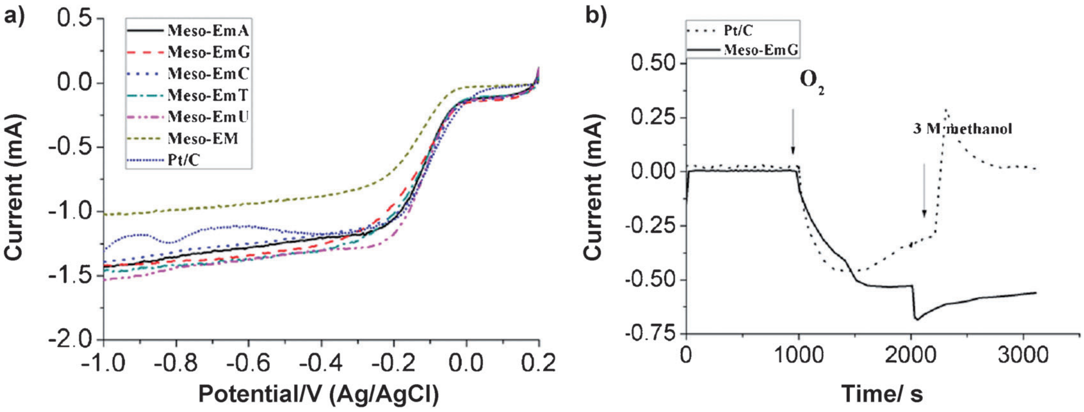

Figure 18. a) Polarization curves on a glassy-carbon rotating-disk electrode for N-doped carbon materials, compared with 20 wt% Pt/C. Conditions: O_2-saturated 0.1 M KOH at a scan rate of 10 mV s^{-1} and rotation rate of 1600 rpm; b) Current–time (*i*–*t*) response of *meso*-EmG and 20 wt% Pt/carbon at −0.26 V in 0.1 M KOH saturated with N_2 (0–1000 s), O_2 (1000–2000 s), and O_2-saturated 3 M CH_3OH (2000–3000 s).[207] (Reproduced with permission from the American Chemical Society, copyright 2010.)

applications, including artificial photosynthesis, oxygenation and reduction reactions, base catalysis, as well as aromatic activation or activation of double and triple bonds. Compared with traditional heterogeneous catalysts or catalyst supports, carbon nitride has many advantages, such as being metal-free, good thermal and chemical stability, tunable electronic structure, and it is abundant and cheap. Therefore, intensified interest can be foreseen in carbon nitride for sustainable chemistry, and further systematic work is needed. The catalytic rates of carbon nitride are still very low when metal-free carbon nitride was used, and this was attributed to the role of covalence in the reversible bonds to be formed and split.

Going forward, we believe that "enzyme-like" multifunctional modifications of carbon nitrides, in particular as functional pores, are a way to improve the performance of metal-free carbon nitride. Another target should be to establish the correlations between the carbon nitride structures and the catalytic activity in relevant reactions. It is still not very clear how carbon nitride interacts with reactants and products and how carbon nitride really influences the relevant reactions. To reach a more fundamental level, a basic understanding of physicochemical properties of carbon nitride is needed.

Another challenge is the extension of domain size and the improvement of electrochemical properties in a traditional semiconductor sense. This is challenging because carbon nitride and its modifications prepared by the bulk condensation route are usually suffer from incomplete polycondensation, which is generally different from batch to batch. As however the organic chemistry of C–N bond formation is very rich, we expect the advent of better, milder, and more reversible synthesis procedures that enable self-organization towards improved structure motifs.

From the perspective of practical applications in sustainable chemistry, only a few reactions have been addressed, essentially proving the required tolerance against multifunctionality and water. Applying this catalyst to specific key reactions and specific substrates will certainly create more exciting results in the near future.

The authors are grateful to the EnerChem project of the Max Planck Society and all the research partners involved in this project. Y.W. thanks the support of the National Natural Science Foundation of China (20806065).

Received: February 16, 2011
Published online: November 23, 2011

[1] J. Dupont, R. F. de Souza, P. A. Z. Suarez, *Chem. Rev.* **2002**, *102*, 3667–3691.
[2] R. E. Galian, J. Perez-Prieto, *Energy Environ. Sci.* **2010**, *3*, 1488–1498.
[3] A. Corma, *Nature* **2009**, *461*, 182–183.
[4] D. R. MacFarlane, K. R. Seddon, *Aust. J. Chem.* **2007**, *60*, 3–5.
[5] P. T. Anastas, M. M. Kirchhoff, *Acc. Chem. Res.* **2002**, *35*, 686–694.
[6] D. E. De Vos, M. Dams, B. F. Sels, P. A. Jacobs, *Chem. Rev.* **2002**, *102*, 3615–3640.
[7] T. Ishida, M. Haruta, *Angew. Chem.* **2007**, *119*, 7288–7290; *Angew. Chem. Int. Ed.* **2007**, *46*, 7154–7156.
[8] G. W. Huber, S. Iborra, A. Corma, *Chem. Rev.* **2006**, *106*, 4044–4098.
[9] X. Huang, X. M. Liu, Q. Luo, J. Q. Liu, J. C. Shen, *Chem. Soc. Rev.* **2011**, *40*, 1171–1184.
[10] A. P. Wight, M. E. Davis, *Chem. Rev.* **2002**, *102*, 3589–3613.
[11] U. Díaz, T. García, A. Velty, A. Corma, *J. Mater. Chem.* **2009**, *19*, 5970–5979.
[12] D. S. Su, J. Zhang, B. Frank, A. Thomas, X. C. Wang, J. Paraknowitsch, R. Schlögl, *ChemSusChem* **2010**, *3*, 169–180.
[13] R. Rinaldi, F. Schüth, *Energy Environ. Sci.* **2009**, *2*, 610–626.
[14] J. V. Liebig, *Ann. Pharm.* **1834**, *10*, 10.
[15] D. J. Benard, C. Linnen, A. Harker, H. H. Michels, J. B. Addison, R. Ondercin, *J. Phys. Chem. B* **1998**, *102*, 6010–6019.
[16] X. J. Bai, C. B. Cao, X. Y. Xu, Q. A. Yu, *Solid State Commun.* **2010**, *150*, 2148–2153.
[17] X. J. Bai, C. B. Cao, X. Y. Xu, *Mater. Sci. Eng. B* **2010**, *175*, 95–99.
[18] R. Wäsche, M. Hartelt, U. Springborn, K. Bewilogua, M. Keunecke, *Wear* **2010**, *269*, 816–825.
[19] M. Naffakh, V. Lopez, F. Zamora, M. A. Gomez, *Soft Mater.* **2010**, *8*, 407–425.
[20] X. Xia, C. H. Zhou, D. S. Tong, M. Liu, D. Zhang, M. Fang, W. H. Yu, *Mater. Lett.* **2010**, *64*, 2620–2623.
[21] T. Tokoroyama, N. Umehara, M. Kamiya, Y. Fuwa, *J. Jpn. Soc. Tribol.* **2010**, *55*, 659–665.
[22] R. V. Shalaev, A. N. Ulyanov, A. M. Prudnikov, G. M. Shin, S. I. Yoo, V. N. Varyukhin, *Phys. Status Solidi A* **2010**, *207*, 2300–2302.
[23] G. F. Jiang, C. H. Zhou, X. Xia, F. Q. Yang, D. S. Tong, W. H. Yu, S. M. Liu, *Mater. Lett.* **2010**, *64*, 2718–2721.
[24] J. C. Byers, P. Tamiasso-Martinhon, C. Deslouis, A. Pailleret, O. A. Semenikhin, *J. Phys. Chem. C* **2010**, *114*, 18474–18480.
[25] I. Banerjee, N. Kumari, A. K. Singh, M. Kumar, P. Laha, A. B. Panda, S. K. Pabi, P. K. Barhai, S. K. Mahapatra, *Thin Solid Films* **2010**, *518*, 7240–7244.
[26] D. G. Liu, J. P. Tu, C. F. Hong, C. D. Gu, S. X. Mao, *Surf. Coat. Technol.* **2010**, *205*, 152–157.
[27] M. Ben Karoui, R. Gharbi, N. Elzayed, M. Fathallah, E. Tresso in *Proceedings of the Jmsm 2008 Conference*, *Vol. 2* (Ed.: A. Cheikhrouhou), **2009**, pp. 873–879.
[28] S. W. Bian, Z. Ma, W. G. Song, *J. Phys. Chem. C* **2009**, *113*, 8668–8672.
[29] E. Kroke, M. Schwarz, *Coord. Chem. Rev.* **2004**, *248*, 493–532.
[30] A. Vinu, *Adv. Funct. Mater.* **2008**, *18*, 816–827.
[31] H. Ito, T. Nozaki, A. Saikubo, N. Yamada, K. Kanda, M. Niibe, H. Saitoh, *Thin Solid Films* **2008**, *516*, 6575–6579.
[32] S. J. Yang, J. H. Cho, G. H. Oh, K. S. Nahm, C. R. Park, *Carbon* **2009**, *47*, 1585–1591.
[33] X. D. Bai, D. Y. Zhong, G. Y. Zhang, X. C. Ma, S. Liu, E. G. Wang, Y. Chen, D. T. Shaw, *Appl. Phys. Lett.* **2001**, *79*, 1552–1554.
[34] Q. A. Li, J. P. Yang, D. Feng, Z. X. Wu, Q. L. Wu, S. S. Park, C. S. Ha, D. Y. Zhao, *Nano Res.* **2010**, *3*, 632–642.
[35] E. Haque, J. W. Jun, S. N. Talapaneni, A. Vinu, S. H. Jhung, *J. Mater. Chem.* **2010**, *20*, 10801–10803.
[36] Z. B. Zhou, R. Q. Cui, Q. J. Pang, G. M. Hadi, Z. M. Ding, W. Y. Li, *Sol. Energy Mater. Sol. Cells* **2002**, *70*, 487–493.
[37] Y. J. Zhang, M. Antonietti, *Chem. Asian J.* **2010**, *5*, 1307–1311.
[38] V. Di Noto, E. Negro, *Electrochim. Acta* **2010**, *55*, 7564–7574.
[39] S. P. Lee, J. G. Lee, S. Chowdhury, *Sensors* **2008**, *8*, 2662–2672.
[40] S. P. Lee, *Sensors* **2008**, *8*, 1508–1518.
[41] A. Thomas, A. Fischer, F. Goettmann, M. Antonietti, J. O. Muller, R. Schlogl, J. M. Carlsson, *J. Mater. Chem.* **2008**, *18*, 4893–4908.

[42] Y. Wang, J. S. Zhang, X. C. Wang, M. Antonietti, H. R. Li, *Angew. Chem.* **2010**, *122*, 3428–3431; *Angew. Chem. Int. Ed.* **2010**, *49*, 3356–3359.

[43] S. C. Yan, Z. S. Li, Z. G. Zou, *Langmuir* **2010**, *26*, 3894–3901.

[44] Y. Miyamoto, M. L. Cohen, S. G. Louie, *Solid State Commun.* **1997**, *102*, 605–608.

[45] E. Horvath-Bordon, E. Kroke, I. Svoboda, H. Fuess, R. Riedel, *New J. Chem.* **2005**, *29*, 693–699.

[46] Y. J. Bai, B. Lu, Z. G. Liu, L. Li, D. L. Cui, X. G. Xu, Q. L. Wang, *J. Cryst. Growth* **2003**, *247*, 505–508.

[47] Y. C. Zhao, Z. Liu, W. G. Chu, L. Song, Z. X. Zhang, D. L. Yu, Y. J. Tian, S. S. Xie, L. F. Sun, *Adv. Mater.* **2008**, *20*, 1777–1781.

[48] M. Groenewolt, M. Antonietti, *Adv. Mater.* **2005**, *17*, 1789—1792.

[49] T. Komatsu, T. Nakamura, *J. Mater. Chem.* **2001**, *11*, 474–478.

[50] X. F. Li, J. Zhang, L. H. Shen, Y. M. Ma, W. W. Lei, Q. L. Cui, G. T. Zou, *Appl. Phys. A* **2009**, *94*, 387–392.

[51] Y. Wang, Y. Di, M. Antonietti, H. R. Li, X. F. Chen, X. C. Wang, *Chem. Mater.* **2010**, *22*, 5119–5121.

[52] M. Antonietti, P. Fratzl, *Macromol. Chem. Phys.* **2010**, *211*, 166–170.

[53] X. C. Wang, K. Maeda, A. Thomas, K. Takanabe, G. Xin, J. M. Carlsson, K. Domen, M. Antonietti, *Nat. Mater.* **2009**, *8*, 76–80.

[54] Y. Wang, H. R. Li, J. Yao, X. C. Wang, M. Antonietti, *Chem. Sci.* **2011**, *2*, 446–450.

[55] S. C. Yan, Z. S. Li, Z. G. Zou, *Langmuir* **2009**, *25*, 10397–10401.

[56] F. Z. Su, S. C. Mathew, G. Lipner, X. Z. Fu, M. Antonietti, S. Blechert, X. C. Wang, *J. Am. Chem. Soc.* **2010**, *132*, 16299–16301.

[57] Y. J. Zhang, A. Thomas, M. Antonietti, X. C. Wang, *J. Am. Chem. Soc.* **2009**, *131*, 50–51.

[58] G. Liu, P. Niu, C. H. Sun, S. C. Smith, Z. G. Chen, G. Q. Lu, H. M. Cheng, *J. Am. Chem. Soc.* **2010**, *132*, 11642–11648.

[59] J. H. Zhang, J. H. Sun, K. Maeda, K. Domen, P. Liu, M. Antonietti, X. Z. Fu, X. C. Wang, *Energy Environ. Sci.* **2011**, *4*, 675–678.

[60] A. V. Semencha, L. N. Blinov, *Glass Phys. Chem.* **2010**, *36*, 199–208.

[61] E. C. Franklin, *J. Am. Chem. Soc.* **1922**, *44*, 486–509.

[62] L. Pauling, J. H. Sturdivant, *Proc. Natl. Acad. Sci. USA* **1937**, *23*, 615–620.

[63] C. E. Redemann, H. J. Lucas, *J. Am. Chem. Soc.* **1940**, *62*, 842–846.

[64] M. L. Cohen, *Phys. Rev. B* **1985**, *32*, 7988–7991.

[65] A. Y. Liu, M. L. Cohen, *Science* **1989**, *245*, 841–842.

[66] M. L. Cohen, *Science* **1993**, *261*, 307–308.

[67] D. M. Teter, R. J. Hemley, *Science* **1996**, *271*, 53–55.

[68] J. L. Corkill, M. L. Cohen, *Phys. Rev. B* **1993**, *48*, 17622–17624.

[69] L. Maya, D. R. Cole, E. W. Hagaman, *J. Am. Ceram. Soc.* **1991**, *74*, 1686–1688.

[70] C. M. Niu, Y. Z. Lu, C. M. Lieber, *Science* **1993**, *261*, 334–337.

[71] D. Marton, K. J. Boyd, A. H. Albayati, S. S. Todorov, J. W. Rabalais, *Phys. Rev. Lett.* **1994**, *73*, 118–121.

[72] K. M. Yu, M. L. Cohen, E. E. Haller, W. L. Hansen, A. Y. Liu, I. C. Wu, *Phys. Rev. B* **1994**, *49*, 5034–5037.

[73] J. P. Rivière, D. Texier, J. Delafond, M. Jaouen, E. L. Mathe, J. Chaumont, *Mater. Lett.* **1995**, *22*, 115–118.

[74] Z. M. Ren, Y. C. Du, Y. X. Qiu, J. D. Nu, Z. F. Ying, X. X. Xiong, F. M. Li, *Phys. Rev. B* **1995**, *51*, 5274–5277.

[75] Y. W. Yang, K. A. Nelson, F. Adibi, *J. Mater. Res.* **1995**, *10*, 41–48.

[76] D. C. Nesting, J. V. Badding, *Chem. Mater.* **1996**, *8*, 1535–1539.

[77] A. Y. Liu, R. M. Wentzcovitch, *Phys. Rev. B* **1994**, *50*, 10362–10365.

[78] J. E. Lowther, *Phys. Rev. B* **1999**, *59*, 11683–11686.

[79] J. Ortega, O. F. Sankey, *Phys. Rev. B* **1995**, *51*, 2624–2627.

[80] M. J. Bojdys, J. O. Müller, M. Antonietti, A. Thomas, *Chem. Eur. J.* **2008**, *14*, 8177–8182.

[81] B. Jürgens, E. Irran, J. Senker, P. Kroll, H. Müller, W. Schnick, *J. Am. Chem. Soc.* **2003**, *125*, 10208–10300.

[82] L. Seyfarth, J. Seyfarth, B. V. Lotsch, W. Schnick, J. Senker, *Phys. Chem. Chem. Phys.* **2010**, *12*, 2227–2237.

[83] A. Sattler, S. Pagano, M. Zeuner, A. Zurawski, D. Gunzelmann, J. Senker, K. Müller-Buschbaum, W. Schnick, *Chem. Eur. J.* **2009**, *15*, 13161–13170.

[84] M. Döblinger, B. V. Lotsch, J. Wack, J. Thun, J. Senker, W. Schnick, *Chem. Commun.* **2009**, 1541–1543.

[85] A. Sattler, W. Schnick, *Z. Anorg. Allg. Chem.* **2008**, *634*, 457–460.

[86] D. R. Miller, J. J. Wang, E. G. Gillan, *J. Mater. Chem.* **2002**, *12*, 2463–2469.

[87] X.-X. Zou, G.-D. Li, Y.-N. Wang, J. Zhao, C. Yan, M.-Y. Guo, L. Li, J.-S. Chen, *Chem. Commun.* **2011**, *47*, 1066–1068.

[88] S. Matsumoto, E. Q. Xie, F. Izumi, *Diamond Relat. Mater.* **1999**, *8*, 1175–1182.

[89] J. Kouvetakis, A. Bandari, M. Todd, B. Wilkens, N. Cave, *Chem. Mater.* **1994**, *6*, 811–814.

[90] C. Li, C. B. Cao, H. S. Zhu, *Mater. Lett.* **2004**, *58*, 1903–1906.

[91] B. V. Lotsch, W. Schnick, *Chem. Mater.* **2006**, *18*, 1891–1900.

[92] Y. Young-Gui, B. G. Pfrommer, F. Mauri, S. G. Louie, *Phys. Rev. Lett.* **1998**, *80*, 3388–3391.

[93] B. Molina, L. E. Sansores, *Mod. Phys. Lett. B* **1999**, *13*, 193–201.

[94] I. Alves, G. Demazeau, B. Tanguy, F. Weill, *Solid State Commun.* **1999**, *109*, 697–701.

[95] Z. H. Zhang, K. Leinenweber, M. Bauer, L. A. J. Garvie, P. F. McMillan, G. H. Wolf, *J. Am. Chem. Soc.* **2001**, *123*, 7788–7796.

[96] M. Mattesini, S. F. Matar, A. Snis, J. Etourneau, A. Mavromaras, *J. Mater. Chem.* **1999**, *9*, 3151–3158.

[97] A. Snis, S. F. Matar, *Phys. Rev. B* **1999**, *60*, 10855–10863.

[98] S. Courjault, B. Tanguy, G. Demazeau, *C. R. Acad. Sci. Ser. IIc* **1999**, *2*, 487–490.

[99] H. Montigaud, B. Tanguy, G. Demazeau, I. Alves, M. Birot, J. Dunogues, *Diamond Relat. Mater.* **1999**, *8*, 1707–1710.

[100] V. N. Khabashesku, J. L. Zimmerman, J. L. Margrave, *Chem. Mater.* **2000**, *12*, 3264–3270.

[101] J. L. Zimmerman, R. Williams, V. N. Khabashesku, J. L. Margrave, *Nano Lett.* **2001**, *1*, 731–734.

[102] E. Kroke, M. Schwarz, E. Horath-Bordon, P. Kroll, B. Noll, A. D. Norman, *New J. Chem.* **2002**, *26*, 508–512.

[103] G. M. Rignanese, J. C. Charlier, X. Gonze, *Phys. Rev. B* **2002**, *66*, 205416.

[104] Y. Zhang, H. Sun, C. F. Chen, *Phys. Rev. B* **2006**, *73*, 144115.

[105] L. Gmelin, *Ann. Pharm.* **1835**, *15*, 252.

[106] J. von Liebig, *Ann. Chem. Pharm.* **1850**, *50*, 337.

[107] J. von Liebig, *Ann. Chem. Pharm.* **1850**, *73*, 257.

[108] H. J. May, *Appl. Chem.* **1959**, 340.

[109] J. Sehnert, K. Baerwinkel, J. Senker, *J. Phys. Chem. B* **2007**, *111*, 10671–10680.

[110] B. V. Lotsch, W. Schnick, *Chem. Eur. J.* **2007**, *13*, 4956–4968.

[111] T. Komatsu, *J. Mater. Chem.* **2001**, *11*, 799–801.

[112] T. Komatsu, *J. Mater. Chem.* **2001**, *11*, 802–805.

[113] A. Sattler, W. Schnick, *Z. Anorg. Allg. Chem.* **2006**, *632*, 238–242.

[114] E. Horvath-Bordon, R. Riedel, P. F. McMillan, P. Kroll, G. Miehe, P. A. van Aken, A. Zerr, P. Hoppe, O. Shebanova, I. McLaren, S. Lauterbach, E. Kroke, R. Boehler, *Angew. Chem.* **2007**, *119*, 1498–1502; *Angew. Chem. Int. Ed.* **2007**, *46*, 1476–1480.

[115] F. Goettmann, A. Fischer, M. Antonietti, A. Thomas, *Angew. Chem.* **2006**, *118*, 4579–4583; *Angew. Chem. Int. Ed.* **2006**, *45*, 4467–4471.

[116] F. Goettmann, A. Fischer, M. Antonietti, A. Thomas, *Chem. Commun.* **2006**, 4530 – 4532.
[117] E. G. Gillan, *Chem. Mater.* **2000**, *12*, 3906 – 3912.
[118] M. Kawaguchi, K. Nozaki, *Chem. Mater.* **1995**, *7*, 257 – 264.
[119] M. Deifallah, P. F. McMillan, F. Cora, *J. Phys. Chem. C* **2008**, *112*, 5447 – 5453.
[120] J. J. Wang, D. R. Miller, E. G. Gillan, *Chem. Commun.* **2002**, 2258 – 2259.
[121] J. S. Zhang, X. F. Chen, K. Takanabe, K. Maeda, K. Domen, J. D. Epping, X. Z. Fu, M. Antonietti, X. C. Wang, *Angew. Chem.* **2010**, *122*, 451 – 454; *Angew. Chem. Int. Ed.* **2010**, *49*, 441 – 444.
[122] M. Zhang, Y. Nakayama, S. Harada, *J. Appl. Phys.* **1999**, *86*, 4971 – 4977.
[123] X. C. Wang, K. Maeda, X. F. Chen, K. Takanabe, K. Domen, Y. D. Hou, X. Z. Fu, M. Antonietti, *J. Am. Chem. Soc.* **2009**, *131*, 1680 – 1681.
[124] S. Polarz, M. Antonietti, *Chem. Commun.* **2002**, 2593 – 2604.
[125] C. D. Liang, K. L. Hong, G. A. Guiochon, J. W. Mays, S. Dai, *Angew. Chem.* **2004**, *116*, 5909 – 5913; *Angew. Chem. Int. Ed.* **2004**, *43*, 5785 – 5789.
[126] A. Thomas, F. Goettmann, M. Antonietti, *Chem. Mater.* **2008**, *20*, 738 – 755.
[127] Y. S. Jun, W. H. Hong, M. Antonietti, A. Thomas, *Adv. Mater.* **2009**, *21*, 4270 – 4274.
[128] X. F. Chen, Y. S. Jun, K. Takanabe, K. Maeda, K. Domen, X. Z. Fu, M. Antonietti, X. C. Wang, *Chem. Mater.* **2009**, *21*, 4093 – 4095.
[129] A. Vinu, K. Ariga, T. Mori, T. Nakanishi, S. Hishita, D. Golberg, Y. Bando, *Adv. Mater.* **2005**, *17*, 1648 – 1652.
[130] X. Jin, V. V. Balasubramanian, S. T. Selvan, D. P. Sawant, M. A. Chari, G. Q. Lu, A. Vinu, *Angew. Chem.* **2009**, *121*, 8024 – 8027; *Angew. Chem. Int. Ed.* **2009**, *48*, 7884 – 7887.
[131] P. Srinivasu, A. Vinu, S. Hishita, T. Sasaki, K. Ariga, T. Mori, *Microporous Mesoporous Mater.* **2008**, *108*, 340 – 344.
[132] M. Antonietti, *Curr. Opin. Colloid Interface Sci.* **2001**, *6*, 244 – 248.
[133] D. H. Chen, Z. Li, Y. Wan, X. J. Tu, Y. F. Shi, Z. X. Chen, W. Shen, C. Z. Yu, B. Tu, D. Y. Zhao, *J. Mater. Chem.* **2006**, *16*, 1511 – 1519.
[134] C. D. Liang, Z. J. Li, S. Dai, *Angew. Chem.* **2008**, *120*, 3754 – 3776; *Angew. Chem. Int. Ed.* **2008**, *47*, 3696 – 3717.
[135] Y. Meng, D. Gu, F. Q. Zhang, Y. F. Shi, L. Cheng, D. Feng, Z. X. Wu, Z. X. Chen, Y. Wan, A. Stein, D. Y. Zhao, *Chem. Mater.* **2006**, *18*, 4447 – 4464.
[136] H. Kosonen, S. Valkama, A. Nykanen, M. Toivanen, G. ten Brinke, J. Ruokolainen, O. Ikkala, *Adv. Mater.* **2006**, *18*, 201 – 205.
[137] Y. Wang, X. C. Wang, M. Antonietti, Y. J. Zhang, *ChemSusChem* **2010**, *3*, 435 – 439.
[138] L. S. Panchakarla, A. Govindaraj, C. N. R. Rao, *Inorg. Chim. Acta* **2010**, *363*, 4163 – 4174.
[139] X. R. Wang, X. L. Li, L. Zhang, Y. Yoon, P. K. Weber, H. L. Wang, J. Guo, H. J. Dai, *Science* **2009**, *324*, 768 – 771.
[140] L. Zhao, N. Baccile, S. Gross, Y. J. Zhang, W. Wei, Y. H. Sun, M. Antonietti, M. M. Titirici, *Carbon* **2010**, *48*, 3778 – 3787.
[141] L. Zhao, X. F. Chen, X. C. Wang, Y. J. Zhang, W. Wei, Y. H. Sun, M. Antonietti, M. M. Titirici, *Adv. Mater.* **2010**, *22*, 3317 – 3321.
[142] Q. Wang, C. C. Chen, W. H. Ma, H. Y. Zhu, J. C. Zhao, *Chem. Eur. J.* **2009**, *15*, 4765 – 4769.
[143] N. Fukata, *Adv. Mater.* **2009**, *21*, 2829 – 2832.
[144] Y. P. Sun, K. F. Fu, Y. Lin, W. J. Huang, *Acc. Chem. Res.* **2002**, *35*, 1096 – 1104.
[145] N. Karousis, N. Tagmatarchis, D. Tasis, *Chem. Rev.* **2010**, *110*, 5366 – 5397.
[146] T. Ouyang, K. P. Loh, D. C. Qi, A. T. S. Wee, M. Nesladek, *ChemPhysChem* **2008**, *9*, 1286 – 1293.
[147] X. C. Wang, X. F. Chen, A. Thomas, X. Z. Fu, M. Antonietti, *Adv. Mater.* **2009**, *21*, 1609 – 1612.
[148] J. J. Zhu, S. A. C. Carabineiro, D. Shan, J. L. Faria, Y. J. Zhu, J. L. Figueiredo, *J. Catal.* **2010**, *274*, 207 – 214.
[149] P. Ritterskamp, A. Kuklya, M. A. Wustkamp, K. Kerpen, C. Weidenthaler, M. Demuth, *Angew. Chem.* **2007**, *119*, 7917 – 7921; *Angew. Chem. Int. Ed.* **2007**, *46*, 7770 – 7774.
[150] S. W. Kohl, L. Weiner, L. Schwartsburd, L. Konstantinovski, L. J. W. Shimon, Y. Ben-David, M. A. Iron, D. Milstein, *Science* **2009**, *324*, 74 – 77.
[151] A. Kudo, Y. Miseki, *Chem. Soc. Rev.* **2009**, *38*, 253 – 278.
[152] F. E. Osterloh, *Chem. Mater.* **2008**, *20*, 35 – 54.
[153] K. Maeda, X. C. Wang, Y. Nishihara, D. L. Lu, M. Antonietti, K. Domen, *J. Phys. Chem. C* **2009**, *113*, 4940 – 4947.
[154] Y. Di, X. C. Wang, A. Thomas, M. Antonietti, *ChemCatChem* **2010**, *2*, 834 – 838.
[155] Q. Y. Li, B. Yue, H. Iwai, T. Kako, J. H. Ye, *J. Phys. Chem. C* **2010**, *114*, 4100 – 4105.
[156] K. Takanabe, K. Kamata, X. C. Wang, M. Antonietti, J. Kubota, K. Domen, *Phys. Chem. Chem. Phys.* **2010**, *12*, 13020 – 13025.
[157] L. Que, W. B. Tolman, *Nature* **2008**, *455*, 333 – 340.
[158] T. Punniyamurthy, S. Velusamy, J. Iqbal, *Chem. Rev.* **2005**, *105*, 2329 – 2363.
[159] A. Corma, H. Garcia, *Chem. Rev.* **2002**, *102*, 3837 – 3892.
[160] I. Hermans, E. S. Spier, U. Neuenschwander, N. Turra, A. Baiker, *Top. Catal.* **2009**, *52*, 1162 – 1174.
[161] Y. Wang, H. R. Li, M. Antonietti, unpublished results.
[162] I. Hermans, P. A. Jacobs, J. Peeters, *Chem. Eur. J.* **2006**, *12*, 4229 – 4240.
[163] F. Li, M. Wang, C. B. Ma, A. P. Gao, H. B. Chen, L. C. Sun, *Dalton Trans.* **2006**, 2427 – 2434.
[164] C. He, J. J. Li, P. Li, J. Cheng, Z. P. Hao, Z. P. Xu, *Appl. Catal. B* **2010**, *96*, 466 – 475.
[165] H. Z. Liu, T. Jiang, B. X. Han, S. G. Liang, Y. X. Zhou, *Science* **2009**, *326*, 1250 – 1252.
[166] N. Herron, C. A. Tolman, *J. Am. Chem. Soc.* **1987**, *109*, 2837 – 2839.
[167] R. Bal, M. Tada, T. Sasaki, Y. Iwasawa, *Angew. Chem.* **2006**, *118*, 462 – 466; *Angew. Chem. Int. Ed.* **2006**, *45*, 448 – 452.
[168] X. F. Chen, J. S. Zhang, X. Z. Fu, M. Antonietti, X. C. Wang, *J. Am. Chem. Soc.* **2009**, *131*, 11658 – 11659.
[169] U. Schuchardt, D. Cardoso, R. Sercheli, R. Pereira, R. S. de Cruz, M. C. Guerreiro, D. Mandelli, E. V. Spinace, E. L. Fires, *Appl. Catal. A* **2001**, *211*, 1 – 17.
[170] T. F. S. Silva, G. S. Mishra, M. F. G. da Silva, R. Wanke, L. Martins, A. J. L. Pombeiro, *Dalton Trans.* **2009**, 9207 – 9215.
[171] M. D. Hughes, Y. J. Xu, P. Jenkins, P. McMorn, P. Landon, D. I. Enache, A. F. Carley, G. A. Attard, G. J. Hutchings, F. King, E. H. Stitt, P. Johnston, K. Griffin, C. J. Kiely, *Nature* **2005**, *437*, 1132 – 1135.
[172] R. E. White, J. T. Groves, G. A. McClusky, *Acta Biol. Med. Ger.* **1979**, *38*, 475 – 482.
[173] G. Smeureanu, A. Aggarwal, C. E. Soll, J. Arijeloye, E. Malave, C. M. Drain, *Chem. Eur. J.* **2009**, *15*, 12133 – 12140.
[174] D. Ferri, A. Baiker, *Top. Catal.* **2009**, *52*, 1323 – 1333.
[175] S. A. Tromp, I. Matijosyte, R. A. Sheldon, I. Arends, G. Mul, M. T. Kreutzer, J. A. Moulijn, S. de Vries, *ChemCatChem* **2010**, *2*, 827 – 833.
[176] D. I. Enache, J. K. Edwards, P. Landon, B. Solsona-Espriu, A. F. Carley, A. A. Herzing, M. Watanabe, C. J. Kiely, D. W. Knight, G. J. Hutchings, *Science* **2006**, *311*, 362 – 365.
[177] R. A. Sheldon, I. Arends, G. J. Ten Brink, A. Dijksman, *Acc. Chem. Res.* **2002**, *35*, 774 – 781.
[178] A. Corma, H. Garcia, *Chem. Soc. Rev.* **2008**, *37*, 2096 – 2126.

[179] Q. Wang, M. A. Zhang, C. C. Chen, W. H. Ma, J. C. Zhao, *Angew. Chem.* **2010**, *122*, 8148 – 8151; *Angew. Chem. Int. Ed.* **2010**, *49*, 7976 – 7979.

[180] M. A. Zhang, C. C. Chen, W. H. Ma, J. C. Zhao, *Angew. Chem.* **2008**, *120*, 9876 – 9879; *Angew. Chem. Int. Ed.* **2008**, *47*, 9730 – 9733.

[181] J. Gawronski, N. Wascinska, J. Gajewy, *Chem. Rev.* **2008**, *108*, 5227 – 5252.

[182] K. C. Nicolaou, C. J. N. Mathison, T. Montagnon, *Angew. Chem.* **2003**, *115*, 4211 – 4216; *Angew. Chem. Int. Ed.* **2003**, *42*, 4077 – 4082.

[183] F. Z. Su, S. C. Mathew, L. Möhlmann, M. Antonietti, X. C. Wang, S. Blechert, *Angew. Chem.* **2011**, *123*, 683 – 686; *Angew. Chem. Int. Ed.* **2011**, *50*, 657 – 660.

[184] C. C. Chen, W. H. Ma, J. C. Zhao, *Chem. Soc. Rev.* **2011**, *39*, 4206 – 4219.

[185] S. C. Yan, S. B. Lv, Z. S. Li, Z. G. Zou, *Dalton Trans.* **2010**, *39*, 1488 – 1491.

[186] Y. Wang, J. Yao, H. R. Li, D. S. Du, M. Antonietti, *J. Am. Chem. Soc.* **2011**, *133*, 2362 – 2365.

[187] S. Watanabe, V. Arunajatesan, *Top. Catal.* **2010**, *53*, 1150 – 1152.

[188] M. Chatterjee, H. Kawanami, M. Sato, A. Chatterjee, T. Yokoyama, T. Suzuki, *Adv. Synth. Catal.* **2009**, *351*, 1912 – 1924.

[189] P. Makowski, R. D. Cakan, M. Antonietti, F. Goettmann, M. M. Titirici, *Chem. Commun.* **2008**, 999 – 1001.

[190] K. K. R. Datta, B. V. S. Reddy, K. Ariga, A. Vinu, *Angew. Chem.* **2010**, *122*, 6097 – 6101; *Angew. Chem. Int. Ed.* **2010**, *49*, 5961 – 5965.

[191] N. Macleod, R. M. Lambert, *Appl. Catal. B* **2002**, *35*, 269 – 279.

[192] J. J. Zhu, Y. C. Wei, W. K. Chen, Z. Zhao, A. Thomas, *Chem. Commun.* **2010**, *46*, 6965 – 6967.

[193] F. Goettmann, A. Fischer, M. Antonietti, A. Thomas, *New J. Chem.* **2007**, *31*, 1455 – 1460.

[194] A. H. Lu, W. Schmidt, N. Matoussevitch, H. Bönnemann, B. Spliethoff, B. Tesche, E. Bill, W. Kiefer, F. Schüth, *Angew. Chem.* **2004**, *116*, 4403 – 4406; *Angew. Chem. Int. Ed.* **2004**, *43*, 4303 – 4306.

[195] M. Groenewolt, A. Thomas, M. Antonietti, *Macromolecules* **2004**, *37*, 4360 – 4364.

[196] C. Laporte, P. Baules, A. Laporterie, J. R. Desmurs, J. Dubac, *C. R. Acad. Sci. Ser. IIc* **1998**, *1*, 141 – 150.

[197] K. P. Gong, F. Du, Z. H. Xia, M. Durstock, L. M. Dai, *Science* **2009**, *323*, 760 – 764.

[198] M. Lefevre, E. Proietti, F. Jaouen, J. P. Dodelet, *Science* **2009**, *324*, 71 – 74.

[199] F. Jaouen, J. Herranz, M. Lefevre, J. P. Dodelet, U. I. Kramm, I. Herrmann, P. Bogdanoff, J. Maruyama, T. Nagaoka, A. Garsuch, J. R. Dahn, T. Olson, S. Pylypenko, P. Atanassov, E. A. Ustinov, *ACS Appl. Mater. Interfaces* **2009**, *1*, 1623 – 1639.

[200] J. P. Paraknowitsch, J. Zhang, D. S. Su, A. Thomas, M. Antonietti, *Adv. Mater.* **2010**, *22*, 87 – 92.

[201] J. P. Paraknowitsch, A. Thomas, M. Antonietti, *J. Mater. Chem.* **2010**, *20*, 6746 – 6758.

[202] J. S. Lee, X. Q. Wang, H. M. Luo, G. A. Baker, S. Dai, *J. Am. Chem. Soc.* **2009**, *131*, 4596 – 4597.

[203] R. Czerw, M. Terrones, J. C. Charlier, X. Blase, B. Foley, R. Kamalakaran, N. Grobert, H. Terrones, D. Tekleab, P. M. Ajayan, W. Blau, M. Ruhle, D. L. Carroll, *Nano Lett.* **2001**, *1*, 457 – 460.

[204] A. C. M. Carvalho, M. C. dos Santos, *J. Appl. Phys.* **2006**, *100*, 084305.

[205] X. Q. Wang, S. Dai, *Angew. Chem.* **2010**, *122*, 6814 – 6818; *Angew. Chem. Int. Ed.* **2010**, *49*, 6664 – 6668.

[206] K. K. R. Datta, W. Balasubramanian, K. Ariga, A. Vinu, *Chem. Eur. J.* **2011**, *17*, 3390 – 3397.

[207] W. Yang, T.-P. Fellinger, M. Antonietti, *J. Am. Chem. Soc.* **2011**, *133*, 206 – 209.